

CREEP BEHAVIOR OF A WOOD-POLYPROPYLENE COMPOSITE

By

RYAN GREGORY KOBBE

A thesis submitted in partial fulfillment of  
the requirements for the degree of

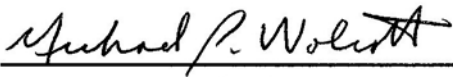
MASTER OF SCIENCE IN CIVIL ENGINEERING

WASHINGTON STATE UNIVERSITY  
Department of Civil and Environmental Engineering

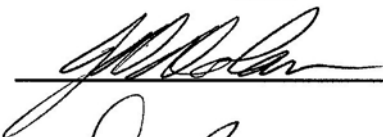
AUGUST 2005


To the Faculty of Washington State University:

The members of the Committee appointed to examine the thesis of  
RYAN GREGORY KOBBE find it satisfactory and recommend that it be  
accepted.

  
\_\_\_\_\_

Chair

  
\_\_\_\_\_

  
\_\_\_\_\_

  
\_\_\_\_\_

# CREEP BEHAVIOR OF A WOOD-POLYPROPYLENE COMPOSITE

## Abstract

by Ryan Gregory Kobbe, M.S.  
Washington State University  
August 2005

Chair: Michael P. Wolcott

Wood-plastic composites offer an inherently durable product well suited for many structural applications. However, their widespread use in engineered applications has been restricted due to a limited understanding of mechanical and time-dependent behavior. The static behavior of this material was evaluated in tension, compression, and flexure. Moment-curvature analysis, utilizing non-linear tensile and compressive constitutive relations, was used to predict the performance and stress distribution of a full-scale flexural member. Short-term creep tests were used to provide insight into the pure mode time-dependent behavior. This test data was also used to infer long-term performance using an accelerated characterization procedure (i.e., TTSSP). It was found that this material exhibits strong non-linear behavior and is sensitive to both the mode and magnitude of the applied load. Findley's stress-independent power law model can be used to accurately represent the creep behavior of this material. At design level stresses, tensile creep impacts the long-term performance of a flexural member more so than compressive creep. Experimental results indicate that this material offers a good balance of strength and stiffness and can be utilized in structural applications if serviceability limitations are addressed. Improvements in section design and/or tensile reinforcement could lead to more efficient material utilization and improved performance.

## TABLE OF CONTENTS

ABSTRACT.....	iii
TABLE OF CONTENTS.....	iv
LIST OF TABLES.....	vii
LIST OF FIGURES .....	ix
CHAPTER 1 – INTRODUCTION .....	1
1.1 Background.....	1
1.2 Incentive.....	2
1.3 Research Development .....	3
1.4 Objectives .....	4
1.5 References.....	6
CHAPTER 2 – EXPERIMENTAL AND ANALYTICAL INVESTIGATIONS OF A STRUCTURAL POLYPROPYLENE WOOD-PLASTIC COMPOSITE .....	8
2.1 Abstract.....	8
2.2 Introduction.....	9
2.3 Analytical Methods.....	10
2.4 Materials and Methods.....	12
2.4.1 Compression .....	13
2.4.2 Tension.....	14
2.4.3 Flexure .....	14
2.5 Results and Discussion .....	15
2.6 Conclusions.....	21

2.7 References.....	22
2.8 Tables.....	25
2.9 Figures.....	29
CHAPTER 3 – TIME-DEPENDENT BEHAVIOR OF A STRUCTURAL POLYPROPYLENE WOOD-PLASTIC COMPOSITE .....	35
3.1 Abstract.....	35
3.2 Introduction.....	36
3.2.1 Creep and Viscoelasticity .....	37
3.3 Analytical Methods.....	38
3.3.1 Findley’s Power Law .....	39
3.3.2 Time-Temperature-Stress Superposition Principle (TTSSP).....	42
3.4 Materials and Methods.....	45
3.5 Results and Discussion .....	46
3.6 Conclusions.....	52
3.7 References.....	54
3.8 Tables.....	57
3.9 Figures.....	61
APPENDIX A – DOWEL BEARING TESTING .....	68
A.1 Introduction.....	68
A.2 Materials and Methods.....	68
A.3 Results and Discussion.....	69
A.4 Conclusions.....	70
A.5 References.....	71

A.6 Tables .....	72
APPENDIX B – COUPON FLEXURE STATIC TESTING .....	73
B.1 Introduction .....	73
B.2 Analytical Methods .....	73
B.3 Materials and Methods .....	74
B.4 Results and Discussion .....	75
B.5 Conclusions .....	76
B.6 References .....	78
B.7 Tables .....	79
B.8 Figures .....	81
APPENDIX C – FLEXURE CREEP TESTING .....	84
C.1 Introduction .....	84
C.2 Analytical Methods .....	84
C.3 Materials and Methods .....	85
C.4 Results and Discussion .....	87
C.5 Conclusions .....	89
C.6 References .....	91
C.7 Tables .....	92
C.8 Figures .....	94

## LIST OF TABLES

Table 2.1. Product details for extruded materials. ....	25
Table 2.2. Extruder temperature profile utilized for all material produced. ....	25
Table 2.3. Average mechanical properties for various loading modes. ....	26
Table 2.4. Maximum strains and constitutive parameters for compression and tension. ....	26
Table 2.5. Measured loads compared to predictions found with constitutive relations. ....	27
Table 2.6. Measured loads compared to predictions found with moment-curvature analysis. ....	28
Table 3.1. Stresses applied in various creep tests ....	57
Table 3.2. Measured strain compared to predictions derived with the general power law. ....	58
Table 3.3. Measured strain compared to predictions derived with Findley's power law. ....	59
Table 3.4. Creep performance at design level stress evaluated 100-min after loading. ....	60
Table 3.5. Coefficients used in the Prony series. ....	60
Table A.1. Dowel-bearing strength data for a PP-based formulation. ....	72
Table B.1. Coupon flexure mechanical properties. ....	79
Table B.2. Measured loads compared to predictions found with moment-curvature analysis. ....	80

Table C.1. Measured strain compared to predictions derived with the general power law.....	92
Table C.2. Measured strain compared to predictions derived with Findley's power law.....	93



## LIST OF FIGURES

Fig. 2.1. Triple box extrusion profile including nominal member dimensions. ....	29
Fig. 2.2. Average stress-strain responses for compression, tension, and flexure. ....	29
Fig. 2.3. Mechanical property comparison for compression, tension, and flexure in a PP-based WPC. ....	30
Fig. 2.4. Modulus comparison for HDPE, PVC, and PP-based WPCs.....	30
Fig. 2.5. Ultimate strength comparison for HDPE, PVC, and PP-based WPCs.....	31
Fig. 2.6. Ultimate strain comparison for HDPE, PVC, and PP-based WPCs.....	31
Fig. 2.7. Constitutive equations fit to compression data.....	32
Fig. 2.8. Constitutive equations fit to tension data. ....	32
Fig. 2.9. Measured load-displacement curves compared with moment-curvature data.....	33
Fig. 2.10. Predicted compressive and tensile outer fiber stress as a function of applied moment.....	33
Fig. 2.11. Location of the neutral axis as a function of applied stress.....	34
Fig. 3.1. Measurements and predictions for creep strain in compression.....	61
Fig. 3.2. Measurements and predictions for creep strain in tension. ....	61
Fig. 3.3. Evaluation of the creep parameters $\varepsilon_0'$ and $\sigma_e$ .....	62
Fig. 3.4. Evaluation of the creep parameters $m'$ and $\sigma_m$ . ....	62
Fig. 3.5. Creep compliance measurements for compression. ....	63
Fig. 3.6. Creep compliance measurements for tension. ....	63
Fig. 3.7. Creep compliance as a function of applied stress.....	64
Fig. 3.8. Creep rate as a function of applied stress. ....	64

Fig. 3.9. Relative creep as a function of applied stress.....	65
Fig. 3.10. The master curve for the creep compliance at 777 psi in compression.....	65
Fig. 3.11. The master curve for the creep compliance at 466 psi in tension.....	66
Fig. 3.12. Variation of stress shift factor with stress difference for compression and tension.....	66
Fig. 3.13. Compliance master curves for compression and tension at 1000 psi.....	67
Fig. B.1. Coupon flexure stress-strain curves.....	81
Fig. B.2. Measured load-displacement curves compared with moment-curvature predictions (coupon flexure).....	82
Fig. B.3. Predicted compressive and tensile outer fiber stress as a function of applied moment (coupon flexure).....	82
Fig. B.4. Location of the neutral axis as a function of applied stress.....	83
Fig. C.1. Measurements and predictions for creep strain in flexure.....	94
Fig. C.2. Evaluation of creep parameters $\epsilon_0'$ and $\sigma_\epsilon$ .....	95
Fig. C.3. Evaluation of creep parameters $m'$ and $\sigma_m$ .....	95
Fig. C.4. Creep compliance measurements for flexure.....	96
Fig. C.5. Creep compliance measurements a various times throughout the test.....	96

# **CHAPTER 1 – INTRODUCTION**

## **1.1 Background**

Wood-plastic composites (WPCs), described as reinforced thermoplastics composed primarily of wood fiber and thermoplastic polymer, have been produced in the United States for several decades. Early building applications were typically restricted to window components (Clemons, 2002). Interest in WPCs has increased significantly in recent years with WPC development growing steadily. Currently, researchers and industries have been developing formulations that exhibit exceptional structural performance characteristics, and many applications that were once constructed with timber elements are being replaced by WPCs (Wolcott, 2001). The increased durability and negligible maintenance requirements of WPCs, when compared to solid wood products, have caused many consumers to view this material favorably (Clemons, 2002; Wolcott and Smith, 2004).

Poor durability can have serious consequences on the safety, serviceability, utility, and visual performance of a structure. Timber structures are particularly vulnerable to damage from moisture, insects, fungi, and ultra violet light (Milner et al., 2000). Despite drawbacks, timber remains the most utilized structural material in America today and is a significant contributor to our economy (Wolcott and Smith, 2004). As a replacement for some timber products, WPCs can meet the consumer's need for a structural material that is durable and cost effective while minimizing environmental costs.

Continued refinement of WPC formulations has lead to the production of a material with exceptional moisture performance, thermal stability, material utilization, and efficiency (Wolcott, 2001). Evaluation of mechanical and performance properties indicates that the future for WPCs include their use in increasingly demanding applications. The evolution of this material will offer engineers and designers the opportunity to utilize complex sections in a variety of structural applications.

## **1.2 Incentive**

The WPC market is well established for use in non-structural applications. Recently, researchers have been working to expand the use of these materials. WPCs have been demonstrated to perform adequately when used as a replacement for treated lumber in marine pier components. Additional projects are also investigating the use of WPCs in light vehicular and pedestrian bridges as well as building components where moisture performance is paramount (e.g. sill plates and foundation connections).

The biggest challenge faced by this emerging industry is societal understanding and acceptance. Wood product development is generally driven by resource availability, resource cost, and proven technology (Rosenberg et al., 1990; Trinka et al., 1992). The ability of the world's forests to continue to supply mature trees suitable for structural applications is diminishing. As a result, the availability of wood has diminished and accordingly its cost has risen (Laver, 1996). Proving that WPC technology is viable appears to be the next step in bringing this material into the regular use in commercial construction.

The mechanical and long-term performance of WPC structural members must be established. From this information, a consistent method for deriving design values can be developed, and serviceability issues can be addressed. The expansion of the WPC market for structural applications is reasonable, provided that viable and acceptable applications can be presented along with procedures for design.

### **1.3 Research Development**

Time dependent deformation of a material under sustained load is referred to as creep. If the load is large and the duration is long, failure (i.e., creep-rupture) will occur. Because WPCs can be subjected to loads over an extended period of time, knowledge of their short-term (static) properties alone may not provide all the information needed to predict long-term performance. It is important, in structures designed to survive decades that progressive deflections be accounted for over the design life. Therefore, the acquisition of creep data and its use in analysis, prediction, and extrapolation are important tasks for materials research.

To account for creep in design, engineers rely on good judgment supported by available models. Many materials display linear viscoelastic behavior over certain ranges of stress, strain, time, and temperature but are non-linear over larger ranges of these variables. Linear viscoelastic behavior has been well documented and a number of constitutive equations have been presented (Findley et al., 1976; Findley, 1960; Flugge, 1967; Fung, 1965). A commonality found in many engineering materials is a non-linear stress-strain relationship combined with properties that are dependent on the loading mode (Altenbach, 2002; Bengtsson, 2000). Non-linear materials continue to be the

subject of ongoing research and a number of articles summarizing attempts to model non-linear viscoelastic response are available (Findley, 1960; Lou and Schapery, 1971; Rand, J.L., 1995; Schapery, 1969). These non-linear materials have constitutive relations that are more complex than linear theory and, therefore, are often derived empirically. For modeling purposes, selecting accurate and mathematically tractable constitutive relations is especially important.

The time-dependant nature of WPCs may have considerable effect on the stress distribution within a member. Given the different creep behavior in compression and tension, the stress and/or strain at any given point within the material may vary significantly with time even though the forces applied are constant. Viscoelastic stress analysis methods are needed to predict the changes in stress/strain distribution over time. Knowledge of time-dependent behavior will allow for the development of complex structural sections, designed to withstand multiple stress states, while exhibiting improved deflection performance.

#### **1.4 Objectives**

This research project will investigate the short-term mechanical behavior of wood-plastic composites (WPCs) subjected to sustained constant stress. WPCs are known to display strain rate effects in response to applied stress. A viscoelastic model is needed to predict the change in stress-strain distribution over time. The nature of a WPC causes creep deflections to become a significant contributor in product serviceability if not properly considered. To mitigate serviceability problems, designers should make every effort to develop a section that can minimize long-term deformations while still

capitalizing on the strength, durability, and economy of these materials. Research has shown that wood-based composite materials exhibit differing strength characteristics under static loadings in various modes (Lockyear, 1999). However, little investigation has been conducted on the creep response of different loading conditions. A more complete understanding of the complex states of stress and strain is needed to fully classify the mechanical behavior of WPC materials. The specific objectives of this research are as follows:

- 1) Establish the static tension and compression behavior for an established wood-polypropylene formulation,
- 2) Examine the static flexure behavior of a structural section using moment-curvature analysis,
- 3) Assess the short-term creep behavior of WPC material in various pure loading modes (i.e., tension and compression). Including establishment of linear/non-linear limits, and
- 4) Investigate the influence of stress level on the material's behavior.

## 1.5 References

- Altenbach, H., "Creep Analysis of Thin-Walled Structures." *Z. Angew. Math. Mech.*, Vol. 82, No. 8, pp. 507-533, 2002.
- Bengtsson, C., "Creep of Timber in Different Loading Modes—Material Property Aspects." World Conference on Timber Engineering, Whistler Resort, British Columbia, Canada, July 31 – August 3, 2000.
- Clemons, C., "Wood-Plastic Composites in the United States, The Interfacing of Two Industries." *Forest Product Journal*, Vol. 52, No. 6., pp. 10-18, 2002.
- Findley, W.N., "Mechanisms and Mechanics of Creep of Plastics." *SPEJ*, Vol. 16, pp. 57-65, January 1960.
- Findley, W.N., Lai, J.S., and Onaran, K., "Creep and Relaxation of Nonlinear Viscoelastic Materials." North-Holland Publishing Company, New York, NY, 1976.
- Flügge, W., "Viscoelasticity." Blaisdell, Waltham, MA, 1967.
- Fung, Y.C., "Foundations of Solid Mechanics." Prentice Hall, Englewood Cliffs, NJ, 1965.
- Laver, T.C., "Extruded Synthetic Wood Composition and Methods for Making Same." Patent Number 5,516,472, 1996.
- Lockyear, S.A., "Mechanical Analysis of Transversely Loaded Wood/Plastic Sections." Master Thesis, Washington State University, December 1999.
- Lou, Y.C. and Schapery, R.A., "Viscoelastic Characterization of a Nonlinear Fiber-Reinforced Plastic," *Journal of Composite Materials*, Vol. 5, pp. 208-234, 1971.
- Milner, M.W., Mettem, C.J., Bainbridge, R.J., and Pitts, G.C., "Considering a Process Approach to Achieving Durability of Timber Structures." World Conference on Timber Engineering, British Columbia, Canada, July 31 – August 3, 2000.
- Rand, J.L., "A Nonlinear Viscoelastic Creep Model." *Tappi Journal*. Pp. 178-182, July 1995.
- Rosenberg, N., Ince, P. Skog, K., and Plantinga, A., "Understanding the Adoption of New Technology in the Forest Product Industry." *Forest Products Journal* 40(10):15-22, 1990.



- Schapery, R.A., "On the Characterization of Nonlinear Viscoelastic Materials." *Polymer Engineering and Science*, Vol. 9, No. 4, pp. 295-310, 1969.
- Trinka, M., Sinclair, S., and Marcin, T., "Determinate Attribute Analysis: A Tool For New Product Development." *Wood Fiber Science* 24(4): 385-391, 1992.
- Wolcott, M.P., "Wood-Plastic Composites." *Encyclopedia of Materials: Science and Technology*, 2001.
- Wolcott, M.P. and Smith, P.M., "Opportunities and Challenges for Wood-Plastic Composites in Structural Applications." *Proceedings of Progress in Woodfibre-Plastic Composites-2004 Toronto, ON*, 2004.

**CHAPTER 2 –**  
**EXPERIMENTAL AND ANALYTICAL INVESTIGATIONS**  
**OF A STRUCTURAL POLYPROPYLENE WOOD-PLASTIC COMPOSITE**

**2.1 Abstract**

The use of thermoplastic composite products in the commercial marketplace has increased rapidly. These naturally durable systems are becoming common in a wide variety of applications not previously considered. Currently, reinforced thermoplastics, such as wood-plastic composites (WPCs), are being investigated for use in structural applications. While development of these materials has progressed significantly, there is still a need to provide relevant mechanical properties for structural design. This paper investigates the static mechanical behavior of a polypropylene-based formulation in compression, tension, and flexure. To characterize this behavior, the non-linear stress-strain relationship must be expressed in usable form. A constitutive model composed of the arc-hyperbolic sine function was found to characterize the pure loading modes (e.g., compression and tension) with acceptable accuracy. The constitutive relations were then used in a moment-curvature analysis to analyze the load-deformation behavior for a full-scale flexural member. This analysis was used to determine stress distribution, moment-curvature relationships, and load displacement behavior in the hollow box-section. This information is essential for the design and development of complex sections intended to maximize the efficiency this material.

## 2.2 Introduction

Use of thermoplastic composites for building construction has recently grown in the commercial market place reaching an estimated \$0.75 billion market in 2004 (Smith and Wolcott, 2005). However, thermoplastic polymers alone frequently lack sufficient strength and stiffness for use in mechanically demanding applications. This has led to the use of synthetic and natural fibers as reinforcing fillers (Nuñez et al., 2003). Reinforced thermoplastics, such as wood-plastic composites (WPCs), offer an inherently durable product that is well suited for many structural applications. The addition of cellulose-based fibers not only reduces costs while improving strength and stiffness, but also improves a number of end-use and processing properties such as thermal stability, UV resistance, and workability (Wolcott, 2001). Commercial production of WPCs typically use thermoplastics such as polyethylene (PE), polyvinyl chloride (PVC), and polypropylene (PP) (Wolcott, 2001). Polypropylene possesses a good combination of physical properties, availability, and reasonable cost, making it a practical choice for many applications. PP is a low-density polymer noted for its good flexural strength, surface hardness, abrasion resistance, and electrical properties (Nuñez, et al., 2003).

WPC development has progressed significantly over the past decade. However, there is a continuing need to establish relevant mechanical, long-term load, and processing performance properties for WPCs composed of different formulations. Testing and analysis has been conducted on formulations composed of a variety of commercially available polymer types. Flexural, compressive, tensile, and dowel bearing performance of PVC and PE-based WPCs has been documented (Adcock et al., 2001; Balma, 1999; Haiar, 2000; Parsons, 2001). More recently, investigations for structural applications

have focused on PP-based WPC formulations (Slaughter, 2004). The work presented here will assist in quantifying the mechanical performance parameters for a PP-based formulation by investigating previously unconsidered loading modes leading to the improved utilization of WPCs in structural applications. The specific objectives are:

- 1) Assess the static behavior of a PP-based WPC in tension, compression, and flexure,
- 2) Provide an appropriate constitutive relationship for modeling of a PP-based composite,
- 3) Verify the load-deformation response of a structural member loaded in flexure with the use of moment-curvature analysis and,
- 4) Evaluate the stress distribution in a beam subjected to design level loads.

### **2.3 Analytical Methods**

Different formulations of WPCs possess significantly different stress-strain relationships depending on the polymer type and form of the reinforcing fiber (Xu et al., 2000; Houshyar and Shanks, 2004; Yang and Chin, 1999). A commonality found in many engineering materials is a non-linear stress-strain relationship combined with properties that are dependent on the loading mode (Altenbach, 2002; Bengtsson, 2000). When deriving the load-deflection behavior of a structural member, one must consider the interaction of the material's inherent behavior in pure loading modes (e.g., tension, compression, and shear). For modeling purposes, selecting accurate and mathematically tractable constitutive relations is especially important. Often, the entire relation must be

used when a material is known to exhibit highly non-linear behavior (Hernandez and Rammer, 1998).

Moment-curvature analysis can accurately determine the load-deformation behavior of an arbitrary section using non-linear stress-strain relationships. The analysis is performed by incrementing the extreme fiber strain until a failure criterion is satisfied. In this case, failure was assumed to occur when a prescribed failure strain is achieved. For each increment, strain is assumed to vary linearly through the cross-section depth, thereby maintaining continuity. The neutral axis is found by iterating until the axial force equilibrium is attained. Finally, the stress distribution in the beam is found using elementary beam theory (more formally known as Euler-Bernoulli Beam Theory). Load, shear, and moment are related to lateral displacement with the following differential expressions:

$$\frac{p}{EI} = \frac{d^4v}{dx^4} \quad (1)$$

$$\frac{-V}{EI} = \frac{d^3v}{dx^3} \quad (2)$$

$$\frac{M}{EI} = \frac{d^2v}{dx^2} \quad (3)$$

where:  $EI$  = flexural rigidity;  $v$  = deflection of the neutral axis;  $p$  = load per unit length;  $V$

= shear force;  $M$  = bending moment;  $\frac{dv}{dx}$  = slope of the beam axis; and  $\frac{d^2v}{dx^2}$  = radius of

curvature (Ugural and Fenster, 2003; Cook et al., 2002).

Structural sections composed of different shapes and materials (i.e., reinforcing) may be investigated by discretizing the shape into layers. The force in each slice is determined by calculating the stress at each location using the assigned constitutive

relation. For linear elastic materials, the measured flexural strength will equal that calculated using simple beam theory. In reality, this is typically not the case and adjustments are made to account for non-uniform stress distribution developed in bending (Laws, 1982). Using a non-linear analysis (i.e., moment-curvature analysis), stress contributions from different compression and tension behavior can also provide valuable insight and facilitate improvements in section design.

## **2.4 Materials and Methods**

Slaughter (2004) identified a polypropylene-based formulation exhibiting superior mechanical, moisture, and extrusion qualities. This optimized formulation maximizes mechanical and physical properties while still providing quality extrusion characteristics (Slaughter, 2004). The formulation is composed of 58.8-percent pine (*Pinus* spp.) flour, 33.8-percent PP, 4.0-percent talc, 2.3-percent maleic anhydride polypropylene (MAPP), and 1.0-percent lubricant by weight. The manufacturer details for each of the material components are provided in Table 2.1. Commercial 60-mesh pine wood (*Pinus* spp.) flour was obtained and dried in a steam tube dryer to a moisture content of approximately 2-percent. Prior to extrusion, the material components were dry blended in powdered form using a 4-ft (1.2-m) drum mixer in a series of 55-lb (25-kg) batches. An 86-mm conical counter-rotating twin-screw extruder (Cincinnati-Milacron TC86) operating at 5 to 12 rpm was used in the production of the required sections. A prearranged screw and barrel temperature profile (Table 2.2) was maintained throughout the extrusion process.

The material evaluated in this research was manufactured in the form of a triple box section with uniform wall thicknesses of 0.4-in. (1.02-cm) using a stranding die

(Laver, 1996). The extruded profile has the nominal outside dimensions of 1.8-in. (5-cm) in depth and 6.5-in. (17-cm) in width (Figure 2.1). All required calculations were performed based on actual dimensions for each specimen, and material originated from a single run, formulation, and section. Modulus of elasticity was defined using the secant method between 5 and 10-percent of ultimate load. The secant modulus is necessary because this material's stress-strain diagram does not exhibit proportionality. In this material, the linear region is restricted to relatively low loads due to the early onset of non-linear behavior.

#### *2.4.1 Compression*

Compressive properties parallel to extrusion direction were established following ASTM D695. Hermanson et al. (1998) indicated that the coupon specimens required by this standard present a gauge length that is too short to allow for accurate deflection measurements. In accordance with these recommendations, an 8.0-in. (20.3-mm) single box section was cut from a full three-box member for testing. Tests of 28 replicates were conducted at a strain rate of 0.01 (in/in)/min ((mm/mm)/min) which corresponded to a crosshead deflection rate of 0.08-in/min (2.03-mm/min). A 30-kip universal electromechanical test machine (Instron 4400R) was utilized for load application, displacement was measured with a 1-inch extensometer (MTS Model 634.12E-24), and data was acquired in real time by computer at 5 Hz. Calculations performed include compressive strength, strain at failure, and modulus of elasticity.

#### 2.4.2 Tension

Tensile properties were established following ASTM D638. Type III dog-bone specimens were cut and milled from the flange of a standard triple box section and machined to a uniform thickness of 0.36-in. (9.19-mm). Tests of 28 replicates were conducted at a strain rate of 0.01 (in/in)/min ((mm/mm)/min) which corresponded to a crosshead deflection rate of 0.08-in/min (2.03-mm/min). A 2-kip universal electromechanical test machine (Instron 4466R) was utilized for load application, displacement was measured with a 1-inch extensometer (MTS Model 634.12E-24), and data was acquired in real time by computer at 5 Hz. Calculations performed include tensile strength, strain at failure, and modulus of elasticity.

#### 2.4.3 Flexure

Full-section flexural properties were established following ASTM D6109. This standard specifies a 16 (+4/-2) support span to depth ratio ( $l/d$ ) for flexure members to minimize the contribution of shear deflections in the beam. However, the relatively low shear areas afforded by hollow sections often result in large flexural shear deflections when compared to solid profiles. To minimize these effects, the test span length was determined using the radius of gyration, rather than the measured depth for the hollow section.

Support span specifications are based on Timoshenko's beam theory (Timoshenko and Goodier, 1987). The form found in ASTM D6109 (i.e.,  $l/d = 16 (+4/-2)$ ) is a simplified representation that allows span length to be defined by the section's depth for a solid rectangular section. In the case of an irregular or multi-celled section, it



is necessary to account for the actual area and moment of inertia, which can be accomplished by representing depth as a function of the radius of gyration. The equivalent  $l/r$  ratio required by this standard is:

$$\frac{l}{r} = 55.4 (+13.9/-6.9) \quad (4)$$

where  $l$  = support span and  $r$  = radius of gyration. For the section considered, the radius of gyration was 0.636-in. (16.15-mm) and requires a support span of 35.25-in. (89.54-cm). The resulting span length was 18-percent longer than that required for a solid section of equal dimensions.

Triple box specimens with 0.4-in. (1.02-cm) wall thickness were tested in third-point bending at a span of 36-in. (0.91-m). Tests of 16 specimens were conducted at an extreme fiber strain rate of 0.01 (in/in)/min ((mm/mm)/min) which corresponded to a crosshead deflection rate of 1.33-in/min (33.8-mm/min). A 30-kip universal electromechanical test machine (Instron 4400R) was utilized for load application. Deflections were measured with a  $\pm 1$ -inch LVDT (Sensotec Corp. Model 060-3618-02, 3.0 VAC). Both load and deflection data was acquired in real time by computer at 2 Hz. Calculations performed include strain at failure, modulus of elasticity (MOE), and modulus of rupture (MOR).

## 2.5 Results and Discussion

Mechanical Properties: Average compressive, tensile, and flexural mechanical properties are summarized in Table 2.3. Modulus values were found to be 652.1, 579.5, and 659.1-ksi (4499, 3995, and 4544-MPa) in compression, tension and flexure, respectively. The corresponding failure strengths and ultimate strains were 8.0, 2.9, and

4.3-ksi (54.8, 20.0, and 29.8-MPa) and 0.0472, 0.0114, and 0.0116-in/in (mm/mm). The modulus values showed the largest variability with the coefficient of variation (COV) ranging from 10 to 22-percent. This variability likely results from the pronounced non-linear nature of the material. COVs associated with this material's ultimate strength ranged from a minimum of 3-percent in compression to a maximum value of 9-percent in tension. Strain at failure COVs were found to be between 8 and 16-percent.

Stress-strain curves from compression, tension, and flexure tests are compared in Figure 2.2. Considering beam theory, the ultimate strength and failure strain in flexure should fall between that of tension and compression, as can be observed in Figure 2.3. The flexural data displayed the most pronounced linear region and possessed a modulus that was within 1-percent of that found for compression. The variability exhibited in tension and compression, indicated as bars in Figures 2.7 and 2.8, may indicate that the load transfer mechanisms vary with mode. While compression tended to have a fairly uniform stress variation with the accumulation of strain, tension displayed very little variation at low strain levels and increased significantly by failure. Figure 2.3 also provides insight into the strength, stiffness and strain relationships that develop in compression and tension. While there is very little change in modulus values, ultimate strength in compression is nearly three-times that found in tension, and ultimate strain was more than four-times greater in compression. Therefore, flexural failures will be initiated in tension.

Mechanical property comparisons assessing this formulation's performance relative to PVC and HDPE-based WPCs by others (Lockyear, 1999; Adcock et al., 2001) are presented in Figures 2.4, 2.5, and 2.6. In general, the PP formulation offers strength

values comparable to those found for PVC while maintaining the ductility of an HDPE formulation. This PP-based formulation appears to provide a good balance of strength, stiffness, and ductility.

Constitutive Modeling: Stress and strain data obtained from compression and tension testing was empirically fit to both hyperbolic tangent and arc-hyperbolic sine functions.

$$\sigma = a \cdot \tanh(b \cdot \varepsilon) \quad (5)$$

$$\sigma = a \cdot \operatorname{asinh}(b \cdot \varepsilon) \quad (6)$$

The constants  $a$  and  $b$  were determined utilizing a least squares minimization technique. The hyperbolic tangent function has been found to fit load-displacement data of WPCs well (Murphy; Lockyear, 1999). The use of hyperbolic sine function relationships has been accepted for relating stress and strain by others (e.g., in the correlation of secondary creep rate (Conway, 1967) and as part of the Findley's (1960) non-linear power law creep model equations). Tensile and compressive maximum strains and constitutive parameters can be found in Table 2.4.

Upon inspection of Figures 2.7 and 2.8, it appears that both hyperbolic tangent and arc-hyperbolic sine functions can be used to characterize the overall compressive and tensile behavior. Compression proved to be the most difficult stress-strain relationship to model consistently because of the large strain range and the highly non-linear stress-strain behavior that occurs even at very low load levels. While the tensile data tended to produce a more uniform fit, both models ranged between the upper and lower bounds of the data. When comparing the relative regions of the curve where the two models tend to fit, they act out of phase with one another. When one model produces an overestimate,

the other tends to underestimate. Overall, both hyperbolic tangent and the arc-hyperbolic sine functions are able to predict the average response with acceptable error and tend to mimic the general non-linear response (Table 2.5).

In this research, investigations will focus on strain levels found for members loaded in flexure, typically less than 0.015 in/in (mm/mm). Therefore, the constitutive models are particularly sensitive to errors in the initial portion of the stress-strain curves. It is noted that the hyperbolic tangent function significantly under-predicts the materials initial stiffness in tension and compression. In comparison, the arc-hyperbolic sine function tends to slightly over-estimate initial stiffness. A constitutive relation composed of the arc-hyperbolic sine function provides the most accurate representation of this material's response particularly in compression during the initial stages of loading. Therefore, all modeling was completed with the use of the arc-hyperbolic sine function.

Moment-Curvature Analysis: Moment-curvature, a one-dimensional beam bending analysis, was used to validate the experimental load-deflection behavior obtained in full-section flexural tests. In this analysis, non-linear tensile and compressive constitutive relations were used to predict the flexural response of the member. The predicted values were then compared with those obtained experimentally. Additionally, the stress distribution throughout the member was evaluated at stresses to failure, as predicted by the maximum strain in either tension or compression.

The analysis was performed, using a Fortran program previously developed by Haiar (2000) for the analysis of flexural members subjected to either 3 or 4-point loading. The program was used to determine stress distribution, moment-curvature relationships, and load displacement behavior accounting for non-linear constitutive relationships. The

analysis was completed considering the following assumptions: (1) plane sections remain plane and (2) only axial stresses and strains act in the material. The use of this program has been proven to provide good predictions of flexural responses (Haiar, 2000).

Prior to analyzing the full-section 3-box specimens, input files were created using average specimen dimensions, test configuration, and the arc-hyperbolic sine constitutive relations. Each section was modeled as an equivalent I-section that was discretized into 43 parallel horizontal layers, 0.04-in. (1.0-mm) thick. Failure was indicated when either the compressive or tensile strain capacity for the material was reached.

Figure 2.9 compares measured and predicted load-displacement curves utilizing this analysis method. Loads estimated with the moment-curvature program were found to be approximately one standard deviation lower than the mean of the experimental data. In general, this analysis is able to capture the shape of the full-section test results, producing load-displacement curves with acceptable accuracy (Table 2.6). Note however, that failure strength and deflection were both under-predicted. Experimental testing produced maximum load and deflection values 11 and 17-percent greater than those obtained from moment-curvature, respectively. Previous researchers have reported calculated bending values falling below experimental observations (Laws, 1982; Haiar, 2000). Law (1982) reported calculated bending values falling below experimental observations and he noted that strain on the tensile face at maximum bending load is often higher than failure strains found in direct tension. He surmised that some of this increase is attributable to the presence of material strength distribution, and he observed that when size effects were included, MOR was predicted with increased accuracy. Additionally, Laws (1982) proposed an analysis technique that accounts for the distribution of flaws on the bending

strength of non-linear materials. Other possible explanations for these differences include: redistribution of energy within the section; the impact of scale on energy redistribution; removal of dense surface material in coupon specimens; and relief of processing stresses during machining. No single cause appears to fully describe the differences observed in strength predictions. All things considered, the results from the moment-curvature analysis are useful in understanding how stresses are distributed within bending members.

Compressive and tensile stresses will not be distributed uniformly in this non-linear material. Figure 2.10 illustrates that as the ultimate load is reached, compressive stress is dominant. Compressive stress at failure was found to be 19-percent greater than tensile stress. Further analysis of the test data indicates that, at stress levels between 30 and 40-percent of the materials ultimate strength, stress in compression is within 4 to 7-percent of that in tension. Therefore, at design stress levels, compressive and tensile forces developed in bending differ by a negligible amount.

The neutral axis of beams in bending may or may not pass through the centroid of the section depending on the relationship between compression and tension that exists. Due to the magnitude of the strength differences exhibited in compression and tension, it was anticipated that the neutral axis would migrate upwards as a result of lower tensile capacity as moment increased. Figure 2.11 shows the neutral axis location as a function of applied load. As the applied moment increased, equilibrium was maintained by the neutral axis shifting away from the tension face. Unsymmetrical flange thickness or reinforcement on the tension face would decrease the neutral axis migration, resulting in lower tensile strain.

## **2.6 Conclusions**

Experimental results presented help establish material properties and stress-strain relationships for a polypropylene based wood-plastic composite. Overall, this material offers a good balance of strength and stiffness. Constitutive relationships using either hyperbolic tangent or the arc-hyperbolic sine functions were found to correlate stress and strain well in tension and compression loading modes. However, the arc-hyperbolic sine function more accurately predicts stresses at low strain levels and is preferred for modeling of materials subjected to moderate stresses. The non-linear flexural behavior of this material can be predicted with reasonable accuracy by moment-curvature calculations. Compressive and tensile stresses contribute similarly in flexure at design level loads (below 40-percent of ultimate). A section design that capitalizes on the compressive strength of this material could significantly increase its load-bearing performance. Thickening of the bottom flange and/or the addition of tensile reinforcement would lead to more efficient material utilization.

## 2.7 References

- Adcock, T., Hermanson, J.C., and Wolcott, M.P., "Engineered Wood Composites for Naval Waterfront Facilities." Washington State University, Project End Report. June, 2001.
- Altenbach, H., "Creep Analysis of Thin-Walled Structures." *Z. Angew. Math. Mech.*, Vol. 82, No. 8, pp. 507-533, 2002.
- ASTM D638-99, "Standard Test Methods for Tensile Properties of Plastics." American Society for Testing and Materials.
- ASTM D695-96, "Standard Test Methods for Compressive Properties of Rigid Plastics." American Society for Testing and Materials.
- ASTM D6109-97, "Standard Test Methods for Flexural Properties of Unreinforced and Reinforced Plastic Lumber." American Society for Testing and Materials.
- Balma, D.A., "Evaluation of Bolted Connections in Wood Plastic Composites." Master Thesis, Washington State University, December 1999.
- Bengtsson, C., "Creep of Timber in Different Loading Modes—Material Property Aspects." World Conference on Timber Engineering, Whistler Resort, British Columbia, Canada, July 31 – August 3, 2000.
- Conway, J.B., "Numerical Methods for Creep and Rupture Analyses." Gordon and Breach, Science Publishers, Inc., New York, NY, 1967.
- Cook, R.D., Malkus, D.S., Plesha, M.E., and Witt, R.J., "Concepts and Applications of Finite Element Analysis." Fourth Edition, John Wiley and Sons, INC., 2002.
- Findley, W.N., "Mechanisms and Mechanics of Creep of Plastics." *SPEJ*, Vol. 16, pp. 57-65, January 1960.
- Haiar, K.J., "Performance and Design of Prototype Wood-Plastic Composite Sections." Master Thesis, Washington State University, May 2000.
- Hermanson, J.C., Adcock, T., and Wolcott, M.P., Evaluation of Extruded Materials Group, "Annual Navy Report ." Washington State University, 1998.
- Hernandez, R. and Rammer, D.R., "Statistical Characterization of Non-linear Elastic Properties." Proceedings from: 5<sup>th</sup> World Conference on Timber Engineering, August 1998.



- Houshyar, S. and Shanks, R.A., "Tensile Properties and Creep Response of Polypropylene Fibre Composites with Variation of Fibre Diameter." *Polymer International*, Vol. 53, pp. 1752-1759, 2004.
- Laver, T.C., "Extruded Synthetic Wood Composition and Method for Making Same." Patent Number 5,516,472. 1996.
- Laws, V., "The Relationship Between Tensile and Bending Properties of Non-linear Composite Materials." *Journal of Materials Science*, Vol. 17, pp. 2919-2924, 1982.
- Lockyear, S.A., "Mechanical Analysis of Transversely Loaded Wood/Plastic Sections." Master Thesis, Washington State University, December 1999.
- Murphy, J.F., "Characterization of Nonlinear Materials." USDA Forest Products Laboratory Technical Note, Madison, WI.
- Núñez, A.J., Sturm, P.C., Kenny, J.M., Aranguren, M.I., Marcovich, N.E. and Reboredo, M.M. "Mechanical Characterization of Polypropylene—Wood Flour Composites." *Journal of Applied Polymer Science*, Vol. 88, pp. 1420-1428, 2003.
- Parsons, W.R., "Energy-Based Modeling of Dowel-Type Connections in Wood-Plastic Composite Hollow Sections." Master Thesis, Washington State University, August 2001.
- Slaughter, A.E., "Design and Fatigue of a Structural Wood-Plastic Composite." Master Thesis, Washington State University, August 2004.
- Smith, P.M. and Wolcott, M.P., "Opportunities and Challenges for WPC's in Emerging Product Areas." *Proceedings to the 8<sup>th</sup> International Conference on Woodfiber-Plastic Composites*, Forest Products Society, Madison, WI, 2005.
- Timoshenko, S.P. and Goodier, J.N., "Theory of Elasticity." McGraw-Hill, Inc, Reissued 1987.
- Ugural, A.C. and Fenster, S.K., "Advanced Strength and Elasticity." Fourth Edition, Prentice Hall, Upper Saddle River, NJ, 2003.
- Wolcott, M.P., "Wood-Plastic Composites." *Encyclopedia of Materials: Science and Technology*, 2001.
- Xu, B., Simonsen, J., and Rochefort, W.E., "Mechanical Properties and Creep Resistance in Polystyrene/Polyethylene Blends." *Journal of Applied Polymer Science*, Vol. 76, pp. 1100-1108, 2000.

Yang, S.W. and Chin W.K., "Mechanical Properties of Aligned Long Glass Fiber Reinforced Polypropylene. II: Tensile Creep Behavior." Polymer Composites, Vol. 20, No. 2, April 1999.

## 2.8 Tables

**Table 2.1.** Product details for extruded materials.

<b>Material</b>	<b>Manufacturer</b>	<b>Product</b>
Polypropylene	Solvay	HB9200
Pine	American Wood Fibers	#6020
Talc	Luzenac	Nicron 403
Coupling Agent	Honeywell	950P
Lubricant	Honeywell	OP100

**Table 2.2.** Extruder temperature profile utilized for all material produced.

<b>Temperature (°F)</b>		
<b>Barrel Zone</b>	1	370
	2	370
	3	365
	4	360
<b>Screw</b>		360
<b>Die Zone</b>	1	360
	2	365
	3	370

**Table 2.3.** Average mechanical properties for various loading modes.

Loading Mode	Modulus	Ultimate Strength	Ultimate Strain
	(psi)	(psi)	(in/in)
Compression	652,128	7,995	0.04716
	(21.5%)	(2.5%)	(15.6%)
Tension	579,454	2,906	0.01142
	(9.5%)	(9.2%)	(8.8%)
Flexure	659,086	4,319	0.01155
	(14.6%)	(6.8%)	(7.8%)

Values in parenthesis indicate associated coefficient of variation.

**Table 2.4.** Maximum strains and constitutive parameters for compression and tension.

		tanh			asinh		
Loading	$\epsilon_{\max}$	a	b	$r^2$	a	b	$r^2$
Tension	0.0114	2984.0	183.0	0.889	1236.9	521.4	0.931
Compression	0.0472	7863.7	56.8	0.822	2566.0	260.3	0.885

**Table 2.5.** Measured loads compared to predictions found with constitutive relations.

Loading Mode	Strain (in/in)	Measured Load <sup>a</sup> (lbs)	Predicted Load (lbs) TANH	Predicted Load (lbs) ASINH	% Difference TANH	% Difference ASINH
Compression	0.0025	4004	2998	4241	-25%	6%
	0.0050	7137	5879	7481	-18%	5%
	0.0100	11416	10922	11677	-4%	2%
	0.0150	14359	14708	14356	2%	0%
	0.0200	16534	17276	16302	4%	-1%
	0.0250	18203	18901	17826	4%	-2%
	0.0300	19457	19883	19077	2%	-2%
	0.0350	20396	20461	20138	0%	-1%
	0.0400	21133	20795	21059	-2%	0%
	0.0450	21579	20987	21872	-3%	1%
	Average Error				6%	2%
Tension	0.0010	144	136	156	-6%	8%
	0.0020	266	264	285	-1%	7%
	0.0030	371	376	384	1%	3%
	0.0040	457	470	462	3%	1%
	0.0050	528	545	526	3%	0%
	0.0060	580	602	580	4%	0%
	0.0070	625	645	626	3%	0%
	0.0080	663	677	667	2%	1%
	0.0090	689	699	703	1%	2%
	0.0100	717	715	735	0%	2%
	Average Error				2%	2%

<sup>a</sup> Average of 28 results

**Table 2.6.** Measured loads compared to predictions found with moment-curvature analysis.

	Deflection (in)	Measured Load <sup>a</sup> (lbs)	Predicted Load <sup>b</sup> (lbs)	% Difference
Full-Section Flexure	0.125	289	264	-8%
	0.250	535	514	-4%
	0.375	764	743	-3%
	0.500	974	947	-3%
	0.625	1167	1129	-3%
	0.750	1340	1292	-4%
	0.875	1496	1438	-4%
	1.000	1637	1570	-4%
	1.125	1764	1690	-4%
	1.250	1877	1800	-4%
	1.375	1975	1901	-4%
	1.500	2055	1974	-4%
	Average Error			-4%

<sup>a</sup> Average of static test results

<sup>b</sup> Moment Curvature Analysis

## 2.9 Figures

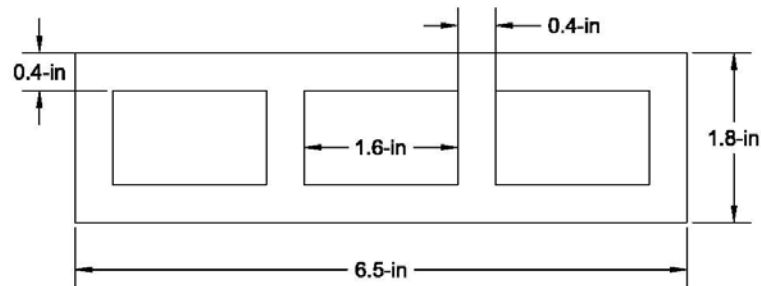


**Fig. 2.1.** Triple box extrusion profile including nominal member dimensions.

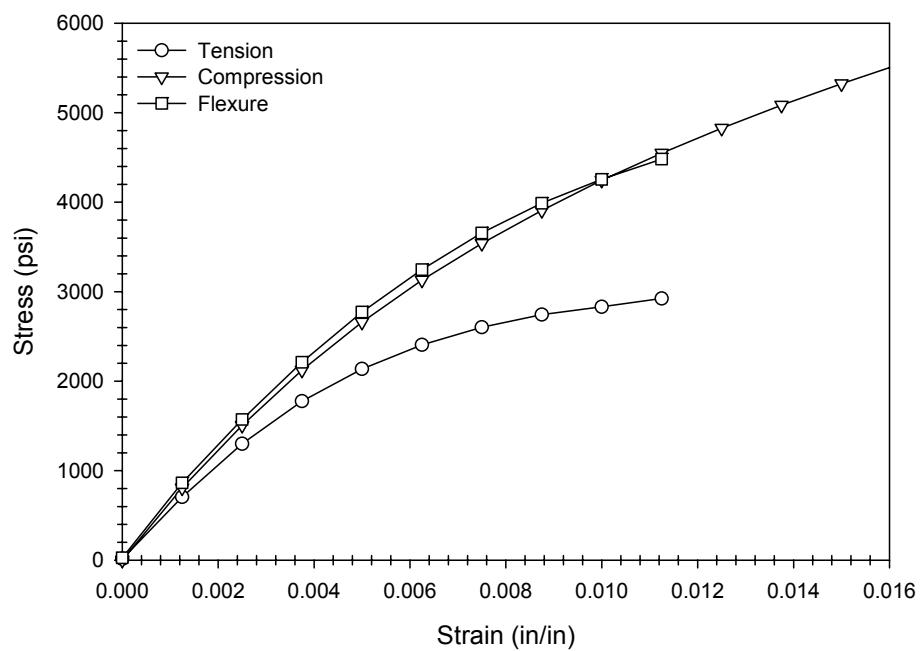


**Fig. 2.2.** Average stress-strain responses for compression, tension, and flexure.

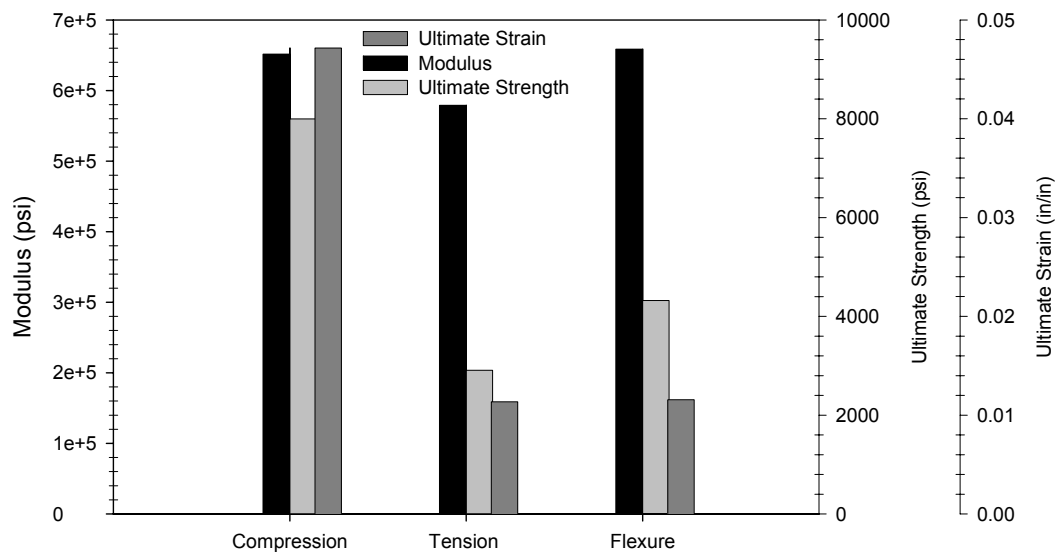


**Fig. 2.3.** Mechanical property comparison for compression, tension, and flexure in a PP-based WPC.

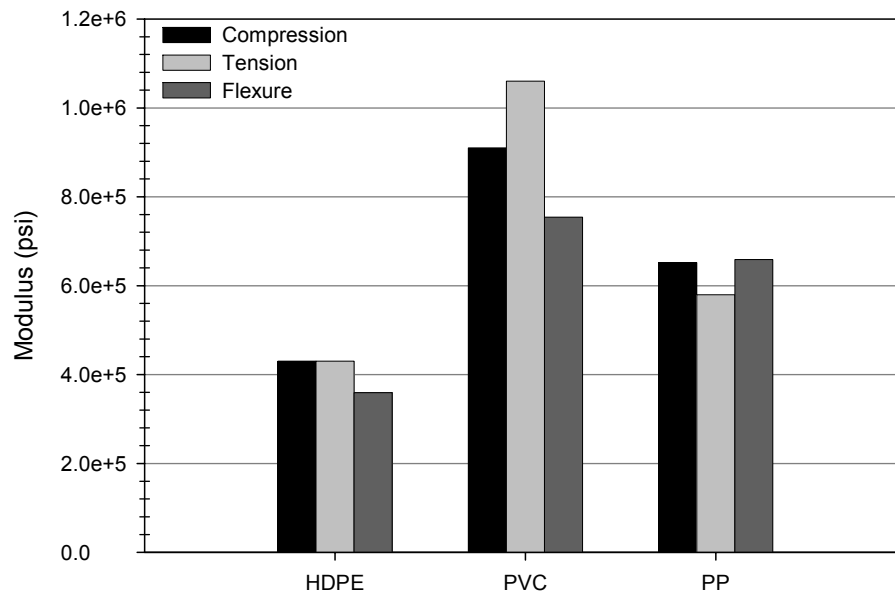


**Fig. 2.4.** Modulus comparison for HDPE, PVC, and PP-based WPCs. (Lockyear, 1999; Adcock et al., 2001)



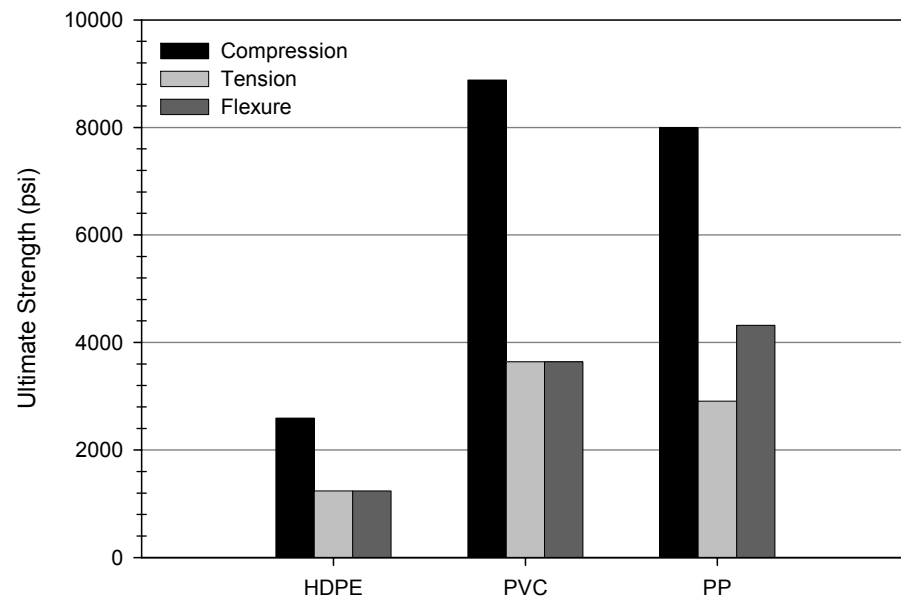


**Fig. 2.5.** Ultimate strength comparison for HDPE, PVC, and PP-based WPCs. (Adcock et al., 2001)

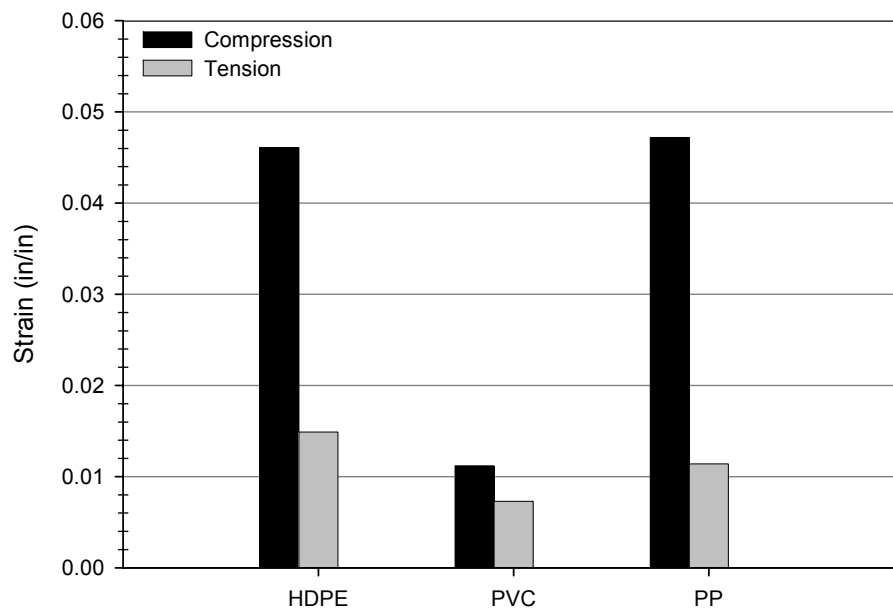


**Fig. 2.6.** Ultimate strain comparison for HDPE, PVC, and PP-based WPCs. (Lockyear, 1999)

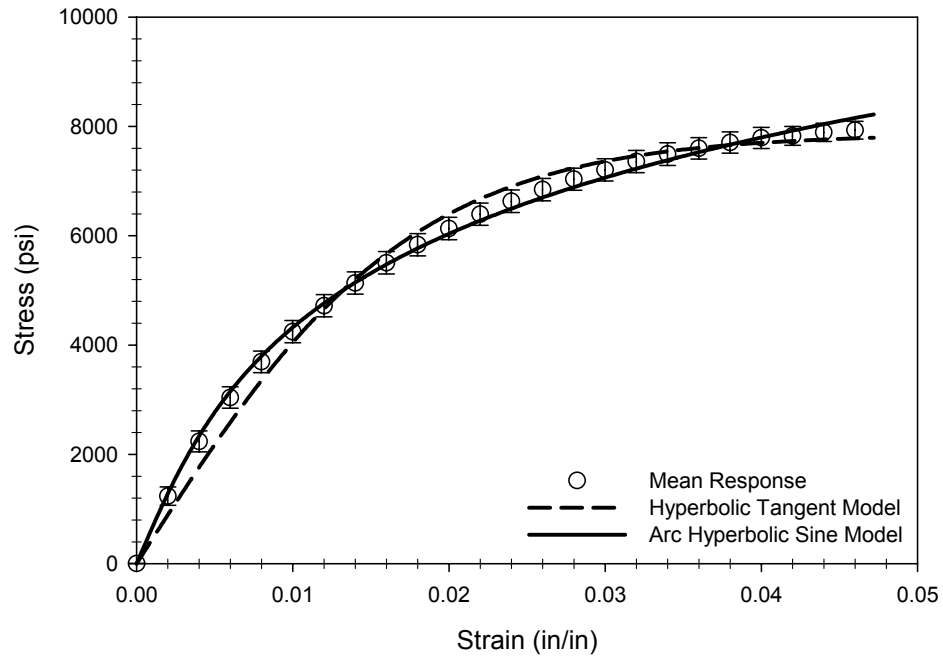


**Fig. 2.7.** Constitutive equations fit to compression data.  
(error bars represent one standard deviation)

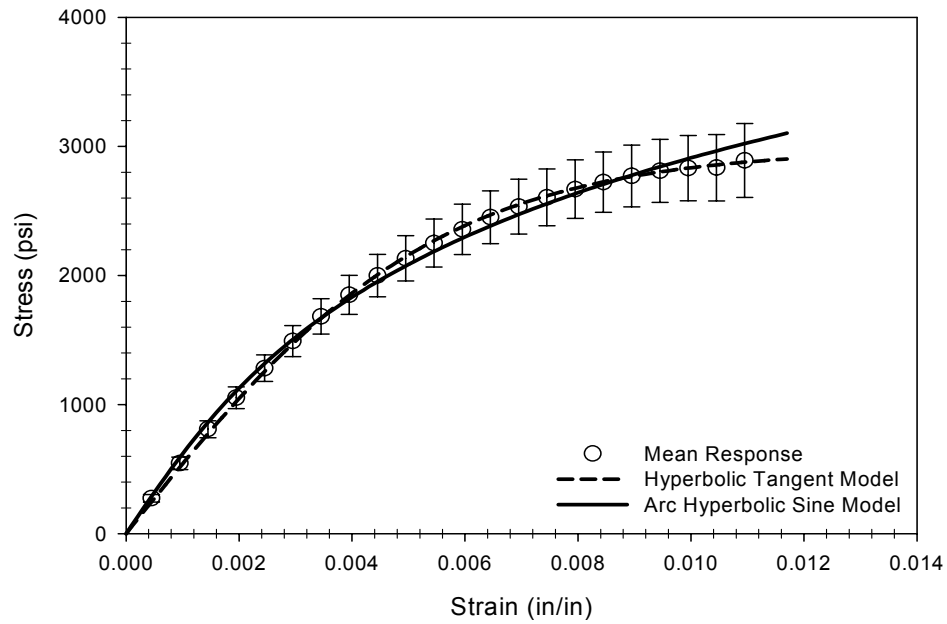


**Fig. 2.8.** Constitutive equations fit to tension data.  
(error bars represent one standard deviation)

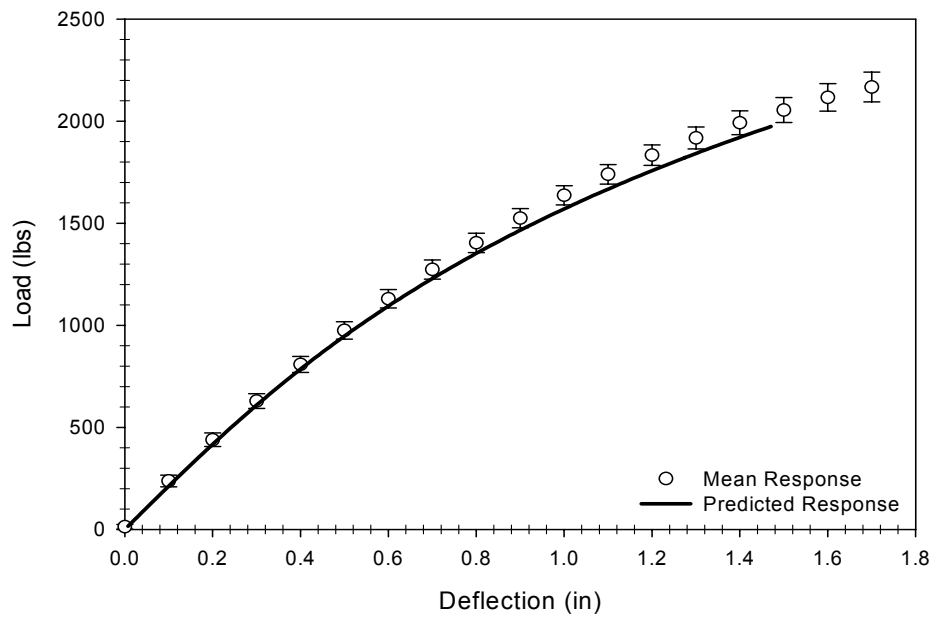


**Fig. 2.9.** Measured load-displacement curves compared with moment-curvature data. (error bars represent one standard deviation)

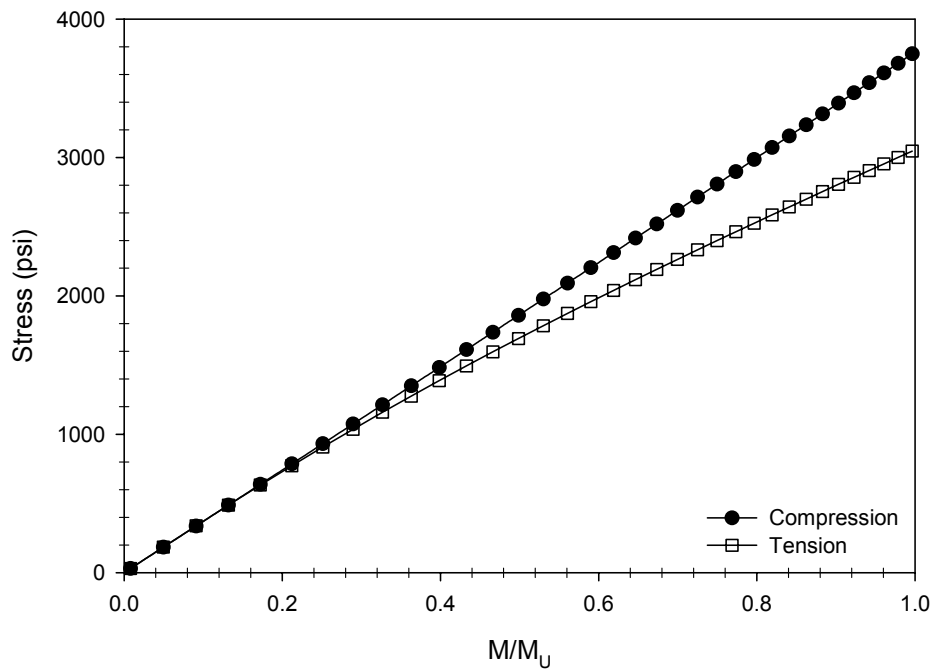


**Fig. 2.10.** Predicted compressive and tensile outer fiber stress as a function of applied moment.

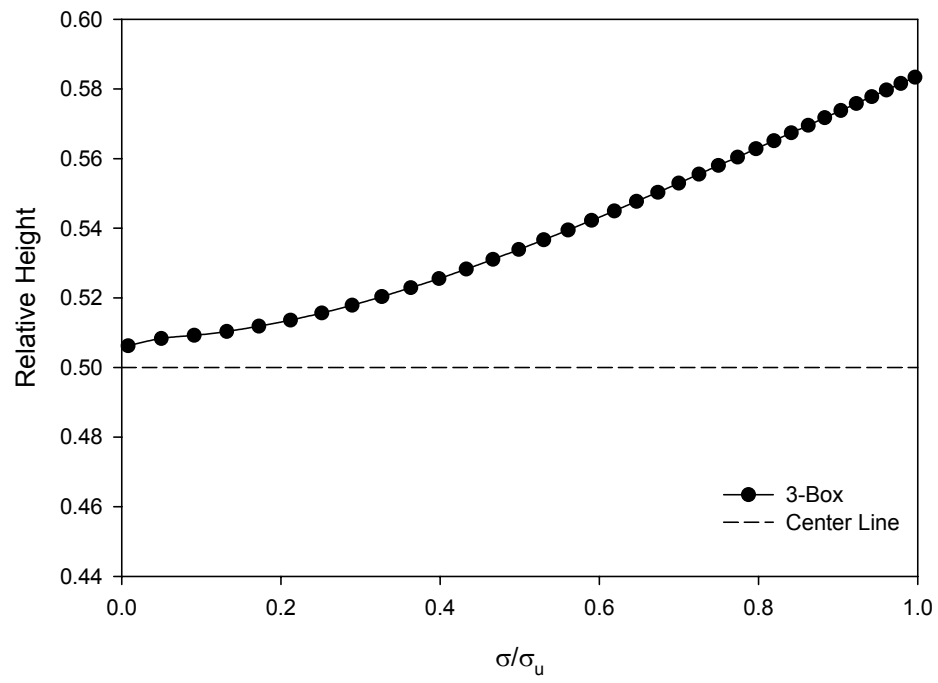


**Fig. 2.11.** Location of the neutral axis as a function of applied stress.

**CHAPTER 3 –**  
**TIME-DEPENDENT BEHAVIOR**  
**OF A STRUCTURAL POLYPROPYLENE WOOD-PLASTIC COMPOSITE**

**3.1 Abstract**

Wood-plastic composites continue to gain acceptance in the conventional building market. However, their widespread usage in structural applications has been restricted due to limited understanding of mechanical behavior. In particular, questions regarding their long-term behavior must be answered. This paper investigates the pure mode creep behavior of a polypropylene-based formulation. The purpose is to provide information that can be used to facilitate the further development of structural wood fiber-reinforced thermoplastics. To account for creep, both empirical and theoretical models are used to describe the material response. Findley's power law accurately predicted the non-linear time-dependent creep deformation of this material with acceptable accuracy. Interpretations of creep compliance curves indicate that this material behaves non-linearly even at stress levels as low as 10-percent of the ultimate stress. Comparisons also indicate that the performance of a flexural member will be most susceptible to long-term performance limitations associated with tensile stresses. Short-term creep data were used to infer long-term performance using an accelerated characterization procedure known as time-temperature-stress superposition (TTSSP). Potentially, the material behavior can be extrapolated to considerably longer time periods using this technique, thus increasing the efficiency with which creep data can be generated.

### 3.2 Introduction

In recent years wood-plastic composites (WPCs) have gained recognition as a viable option to conventional building materials in weathering applications. Mainstream use of WPCs in engineered applications has been restricted due, in part, to a limited understanding of mechanical behavior. Despite improved processing methods and mechanical properties, investigations into long-term structural performance characteristics of WPCs are limited.

Knowledge of a material's mechanical behavior and the ability to describe the behavior mathematically will strongly impact the accuracy of structural analysis performed in practice. In applications demanding long-term structural performance (e.g., beams, columns, floor and roof systems) creep and creep rupture considerations are critical (Alvarez et al., 2004). Excessive deflections are avoided in design codes by considering deflections in a structure for its expected service life. For polymeric materials, creep can contribute significantly in deflection calculations. When appropriate creep models are unavailable, designers account for long-term reductions in stiffness by reducing the modulus of elasticity with a creep factor. Additionally, to avoid failure (i.e., creep rupture) of a structural member, design codes require that static strength values be reduced to account for duration of load effects. Therefore, acquisition of creep data and its use in analysis, prediction, and extrapolation are important tasks for materials research.

This paper presents the principal results of a study on creep behavior of a polypropylene-based WPC loaded in tension and compression. Knowledge of time-dependent behavior will facilitate the development of complex structural sections,

designed to withstand multiple stress states, which exhibit improved deflection performance. The specific objectives are:

- 1) Assess the short-term creep behavior of the WPC material in tension and compression,
- 2) Investigate the influence of stress level on the linear/non-linear behavior of this material in tension and compression,
- 3) Provide an appropriate constitutive relation for modeling of a PP-based composite and,
- 4) Assess time-stress superposition techniques as possible accelerated testing methods for creep evaluation.

### *3.2.1 Creep and Viscoelasticity*

Because WPCs are composed of a polymer matrix reinforced by short-fibers, significant time-dependent behavior may be expected (Findley, 1960; Mallick, 1988). Viscoelastic deformation (i.e., creep) of polymers occurs as a combination of elastic and time-dependent deformation. The linear polymer chains of the thermoplastic matrix are particularly susceptible to long-term deformation processes (Findley, 1960; Wolcott and Smith, 2004). At high stress levels, this behavior may become non-linear or stress dependent and, therefore, more complex to describe (Papanicolaou et al., 1999). When the applied stresses are sufficiently small and have negligible effect on the material's properties, a linear viscoelastic representation is acceptable. However, at higher stresses, most polymers exhibit non-linear viscoelastic behavior (Jazouli et al., 2005).

A number of investigations have been completed on the time-dependent behavior of thermo-set composites. However, works that specifically compare the pure mode creep behavior of WPCs are limited. Sain et al. (2000) investigated load, time, and temperature effects for PVC, PE, and PP-based WPCs loaded in flexure. Nuñez et al. (2004) described the effects of wood flour content, interface treatments, and temperature on the time-dependent behavior of a PP-wood composite using the Burgers model and a power law equation. Testing on a multi-celled commercial decking product completed by Lin et al. (2004) attempted to determine the creep related material constants for HDPE samples in order to simulate flexural creep data. This research is intended to investigate the creep response on a WPC loaded in various pure modes (i.e., compression and tension) in order to more fully understand the complex state of stress that develops in bending.

### **3.3 Analytical Methods**

To account for creep in design, engineers depend on good judgment supported by available models. A number of empirical and theoretical methods have been developed to express time-dependent creep strains. Various researchers have investigated modeling both linear and non-linear viscoelastic materials. Linear viscoelastic behavior has been well documented and a number of constitutive equations have been presented (Findley et al., 1976; Findley, 1960; Flugge, 1967; Fung, 1965). Non-linear materials continue to be the subject of ongoing research and a number of articles summarizing attempts to model non-linear viscoelastic response are available (Findley, 1960; Lou and Schapery, 1971; Rand, 1995; Schapery, 1969). While phenomenological models can be helpful in interpreting and predicting observed creep behavior, these models are only valid for



conditions within the range of those studied. It is necessary to demonstrate that the actual material behavior is consistent with that of the model when using these models outside the conditions studied.

Industrial applications of WPCs will necessitate long-term performance and new products must demonstrate appropriate behavior. To reduce the expense and time necessary to generate long-term creep information for design purposes, methods for extrapolating and interpolating experimental data are needed. Accelerated characterization procedures provide techniques to forecast a material's response, and information on long-term deformation and strength is normally obtained by extrapolation of short-term test data, obtained under accelerated testing conditions. Accelerating factors that have been derived from fundamental thermodynamics of material behavior include temperature, stress, and humidity. The accelerated characterization method used in this study is time-temperature-stress superposition principle. It is important to remember that the accelerating factor can only be used if it does not change the mechanism controlling creep at ambient conditions.

### *3.3.1 Findley's Power Law*

A reliable and widely recognized creep model was needed to evaluate the time-dependent deformation of WPCs tested in this study. The creep model used here is the power law proposed by Findley (Findley et al., 1976; Findley, 1960). This model is reasonably simple and has been proven to apply to a variety of viscoelastic materials loaded at moderate levels, including fiber reinforced plastics. Shao and Shanmugam (2004) used a simplified Findley model to obtain the time-dependent shear and tensile

moduli of a pultruded composite sheet piling. Choi and Yuan (2003) found this model was able to successfully predict time-dependent deformations of glass fiber reinforced columns. Park and Balatinecz (1998) used it to investigate the effects of wetting agent, temperature, and wood-fiber concentration in a polypropylene-based WPC. In addition, this model has been validated by creep tests with a total duration of up to 26 years (Findley, 1987). In this research, Findley's power law model was used to describe non-linear creep because the phenomenological approach is descriptive, mathematically simplistic, and widely accepted.

The general form of Findley's power law is given as:

$$\varepsilon_t = \varepsilon_0 + m \left( \frac{t}{t_0} \right)^n \quad (1)$$

where:  $\varepsilon_t$  = time dependent creep strain;  $\varepsilon_0$  = instantaneous strain;  $m$  = coefficient of time-dependent strain;  $n$  = exponential material constant;  $t$  = time after loading; and  $t_0$  = unit time. In this form, both  $\varepsilon_0$  and  $m$  are dependent on applied stresses, while  $n$  is typically independent. This equation describes creep behavior of a particular material at a given stress level and temperature.

To describe creep behavior of a material at any stress level, the stress dependent model parameters ( $\varepsilon_0$ ,  $m$ ) can be replaced by hyperbolic functions (Findley, 1960):

$$\varepsilon_0 = \varepsilon'_0 \sinh \left( \frac{\sigma}{\sigma_\varepsilon} \right) \quad (2)$$

$$m = m' \sinh \left( \frac{\sigma}{\sigma_m} \right) \quad (3)$$

where:  $\varepsilon_0'$  = instantaneous strain at the reference stress level  $\sigma_\varepsilon$ ;  $\sigma$  = applied stress;  $m'$  = creep parameter  $m$  at the reference stress level  $\sigma_m$ . Replacing  $\varepsilon_0$  and  $m$  in Equation (1) with these hyperbolic expressions, the power law can be written as follows,

$$\varepsilon_t = \varepsilon_0' \sinh\left(\frac{\sigma}{\sigma_\varepsilon}\right) + m' \sinh\left(\frac{\sigma}{\sigma_m}\right) \left(\frac{t}{t_0}\right)^n \quad (4)$$

The constants  $\varepsilon_0'$ ,  $\sigma_\varepsilon$ ,  $m'$ , and  $\sigma_m$  are empirically determined from data collected at different stress levels. Values for  $\sigma_\varepsilon$  and  $\sigma_m$  are determined by linearizing the curves for  $\varepsilon_0$  and  $m$  obtained in tests over a range of stresses. Note that these parameters are independent and therefore, not necessarily equal. Values for  $\varepsilon_0'$  and  $m'$  are taken as the slope of a straight-line fit through the respective data with the use of a least squares fit procedure. The value obtained for  $\varepsilon_0'$ ,  $\sigma_\varepsilon$ ,  $m'$ ,  $\sigma_m$ , and  $n$  are all constants that are independent of stress, strain, and time but; these parameters remain a function of the material, temperature, humidity, and other environmental factors.

Findley's power law model is only valid for materials that undergo primary creep as characterized by a decreasing creep rate over time. At higher stress levels, creep-rate will reach a monotonic state or increase leading to secondary and tertiary creep stages, respectively. Therefore, the hyperbolic sine function can be used to describe stress dependence only for moderate values of stress. The Findley power law has been shown to be an adequate model for materials similar to those being investigated in this report up to approximately 50 to 60-percent of its ultimate strength (Scott and Zureick, 1998; Choi and Yuan, 2003; Sain et al., 2000).

### *3.3.2 Time-Temperature-Stress Superposition Principle (TTSSP)*

Designing for creep deformation requires the collection of data over long periods of time, which is costly and often impractical. Founded on the superposition theory of viscoelasticity, long-term creep behavior can be predicted from short-term data using an accelerated characterization procedure. Increased stress accelerates creep of many viscoelastic materials, similar to the effect from increased temperature. A number of researchers have proposed time-temperature-stress superposition principles (TTSSP) (Schapery, 1969; Yen and Williamson, 1990; Brinson et al., 1978). The fundamental ideas behind TTSSP are: (1) particular environmental conditions such as temperature and stress level can accelerate the viscoelastic deformation process; (2) the creep deformation curves associated with different conditions are of the same shape; (3) an increase in temperature or stress will shift creep deformation curves on a log-time scale; and (4) these curves can be combined to form a smooth continuous curve, known as the master curve. When successful, the master curve formed using TTSSP, represents the predicted long-term viscoelastic response at a given reference condition.

Time-temperature-stress superposition assumes that creep behavior at one temperature or stress can be related to that at another by simply shifting the data along the log-time scale. This shift implies that as temperature or stress increases, molecular relaxations accumulate at a constant rate and that the underlying mechanism of creep remains unchanged. Free volume theory is often used to describe this molecular mobility. Free volume is viewed as void space allowing motion of polymer chains. Time-dependent mechanical properties can be directly related to changes in free volume

(Knauss and Emri, 1981). Wenbo et al. (2001) proposed a TTSSP that is construed within the framework of free volume theory. The following discussion summarizes their work.

From free volume theory, the viscosity of a material,  $\eta$ , can be related to the free volume fraction,  $f$  by:

$$\ln \eta = \ln A + B \left( \frac{1}{f} - 1 \right) \quad (5)$$

where  $A$  and  $B$  = material constants. Equation (5), known as the Doolittle equation, is the foundation of time-temperature superposition.

Assuming that changes in the free volume fraction are linearly dependent on stress changes, as well as temperature changes, the free volume fraction as a function of temperature and stress can be expressed as:

$$f = f_0 + \alpha_T (T - T_0) + \alpha_\sigma (\sigma - \sigma_0) \quad (6)$$

where:  $\alpha_T$  = coefficient of thermal expansion;  $\alpha_\sigma$  = stress-induced expansion coefficient of the free volume fraction; and  $f_0$  = free volume fraction at a reference temperature and stress.

Presume there exists a shift factor ( $a_{T\sigma}$ ) that satisfies

$$\eta(T, \sigma) = \eta(T_0, \sigma_0) a_{T\sigma} \quad (7)$$

then Equations (5) and (6) can be combined:

$$\log(a_{T\sigma}) = -C_1 \left[ \frac{C_3(T - T_0) + C_2(\sigma - \sigma_0)}{C_2 C_3 + C_3(T - T_0) + C_2(\sigma - \sigma_0)} \right] \quad (8)$$

where  $C_3 = f_0 / \alpha_\sigma$ .

Additionally, the stress shift factor at constant temperature  $a_\sigma^T$  and the temperature shift factor at constant stress level  $a_T^\sigma$  are defined so that

$$\eta(T, \sigma) = \eta(T, \sigma_0) a_\sigma^T = \eta(T_0, \sigma_0) a_\sigma^T a_T^{\sigma_0} = \eta(T_0, \sigma) a_T^\sigma = \eta(T_0, \sigma_0) a_\sigma^{T_0} a_T^\sigma \quad (9)$$

therefore,

$$a_{T\sigma} = a_\sigma^T a_T^{\sigma_0} = a_\sigma^{T_0} a_T^\sigma \quad (10)$$

Equation (10) shows that time-dependent properties of viscoelastic materials at different temperatures and stress levels can be shifted along the time scale to construct a master curve of a wider time scale at a given temperature,  $T_0$ , and stress level,  $\sigma_0$ .

In a case where service temperature is chosen as the reference temperature,  $T_0$ , Equation (8) reduces to:

$$\log(a_{T\sigma}) = -C_1 \left[ \frac{C_1(\sigma - \sigma_0)}{C_3 + (\sigma - \sigma_0)} \right] \quad (11)$$

where  $a_\sigma$  = stress shift factor. Now non-linear creep compliance at varied stress levels can be related by the reduced time,  $t/a_\sigma$ .

$$J(\sigma, t) = J\left(\sigma_0, \frac{t}{a_\sigma}\right) \quad (12)$$

TTSSP has been found to be a valid method to generate a master curve that can be used to predict long-term creep. Lai and Bakker (1995) used this technique to investigate the distribution of relaxation times of HDPE. Ma et al. (1997) examined the accelerated characterization of the creep responses for laminated composites due to the effects of temperature and stress. A stress-time superposition procedure was found to successfully extend creep data generated on glass-reinforced polypropylene composite (Cessna, 1971). In this research, the procedure for extending non-linear creep data is considered because the approach is reasonably simplistic and widely acknowledged.

An analytical expression is needed to represent the compliance of the superposed master curve. Spring and dashpot models are often used to describe complex viscoelastic

behavior (Flugge, 1967; Findley et al., 1976). The versatility of these models is due to their ability to include additional stiffness and damping terms needed to describe mode changes in long-duration tests. One such model, a representation composed of a series of decaying exponentials, commonly known as a Prony series, is well established (Park and Kim, 2001). The popularity of this model is primarily due to its computational efficiency. The Prony series is stated mathematically as:

$$\bar{J}(t) = J_0 + \sum_{i=1}^N J_i \left[ 1 - e^{-t/\tau_i} \right] \quad (13)$$

where:  $J_0$  = instantaneous compliance;  $J_i$  = compliance constant;  $\tau_i$  = retardation time constant; and  $i$  = element number in series ( $i = 1, 2, \dots$ ).

### 3.4 Materials and Methods

Short-term tests were performed to assess creep response of a WPC formulation in both tensile and compressive modes. All specimens were composed of a polypropylene (PP) based formulation consisting of 58.8% pine (*Pinus* spp.) flour (60-mesh, Amercian Wood Fibers 6020), 33.8% polypropylene (PP) matrix resin (Solvay HB9200), 4% talc (Luzenac Nicron 403), 2.3% maleic anhydride polypropylene (MAPP) coupling agent (Honeywell 950P), and 1.0% lubricant (Honeywell OP100) by weight. Triple box, hollow sections were extruded with an 86-mm conical twin-screw extruder using a stranding die (Laver, 1996). The extruded profile has a nominal wall thickness of 0.4-in. (1.02-cm) with nominal outside dimensions of 1.8-in. (5-cm) depth and 6.5-in. (17-cm) width, and material originated from a single run, formulation, and section.. Specimens were machined to size and environmentally conditioned at 70° F (21.1° C) and 50-percent RH. Testing was performed in an environmentally conditioned room controlled to 70° F

(21.1° C) and 50-percent RH. Loads were applied with a 22-kip servo-hydraulic load frame (MTS 810), displacement measurements were taken with a 1-inch extensometer (MTS Model 634.12E-24), and data was acquired in real time by computer at 1 Hz.

The modulus of rupture (MOR) values, obtained from static testing, were used as a reference stress level to determine the applied creep loads. To facilitate proper comparisons, coupon specimens were prepared to match those evaluated in static testing. Compression specimens consisted of an 8-in. single box section cut from a full three-box member as described by Kobbe (2005). Tension specimens were cut from the flange of a triple-box section and machined to a uniform thickness of 0.35-in. (8.89-mm). Type III dog-bone samples were then machined on a shaper table in conformance with ASTM D638.

The creep tests consisted of applying controlled levels of stress using a servo-hydraulic, universal test machine set to operate in load-control. Loads were applied to eight replicate specimens for each stress level and loading mode (tension and compression). Applied loads resulted in stress levels ranging from approximately 10 to 60-percent of the ultimate static strength. This range exceeded the anticipated design stresses in structural applications. The stresses applied in each test are reported in Table 3.1. During testing, each specimen was loaded to the prescribed stress level in approximately 1-second and this load was maintained for 100-minutes.

### **3.5 Results and Discussion**

The experimental and theoretical creep curves are presented in Figures 3.1 and 3.2 for compression and tension, respectively. Predictions presented in the figures are



formulated using both the general form of the power law (Equation (1)) as well as the stress independent model (Equation (4)) developed by Findley.

Constitutive Modeling: The general power law model fit the creep parameters  $m$  and  $n$  to experimental data at each stress level. To facilitate a consistent model evaluation, the initial strain,  $\varepsilon_0$ , was taken as the strain recorded 4-seconds following load application. The values for the model parameters are given in Table 3.2, along with both experimental and predicted strains at selected times. It can be seen that the results are in general agreement with predictions deviating by less than 1-percent from experimental findings.

The creep parameter,  $n$ , showed little variability among the stress levels and loading modes, averaging  $0.281 \pm 3.0\%$  and  $0.300 \pm 6.4\%$ , for compression and tension, respectively. These results suggest that differences are negligible, for modeling purposes, and  $n$  can be taken as a single value. In contrast, values for the creep parameters,  $m$  and  $\varepsilon_0$ , varied considerably with stress level. As discussed previously, these stress dependent model parameters can be replaced under moderate stress by hyperbolic functions (Equations (2) and (3)). The constants  $\varepsilon_0'$ ,  $\sigma_\varepsilon$ ,  $m'$ , and  $\sigma_m$  are empirically determined from data collected at different stress levels. Values for  $\sigma_\varepsilon$  and  $\sigma_m$  were determined by linearizing the curves for  $\varepsilon_0$  and  $m$  obtained in tests over a range of stresses. Values for  $\varepsilon_0'$  and  $m'$  were taken as the slope of a straight-line fit through the respective data (Figures 3.3 and 3.4). Table 3.3 shows values for the stress independent Findley power law model as well as predictions at selected times. Equation (4) was used to estimate creep strains at various loading levels within the bounds of the experimental data. Differences between experimental and estimated values were typically less than 10-percent. Exceptions were

found at low stress levels where the magnitude of the applied stress is low in relation to the range of the model.

When observing the model fit to the mean creep curves plotted in Figures 3.1 and 3.2, note that Findley's model begins to diverge from measured data as the applied stress level reaches or exceeds 60-percent of the ultimate stress. This result is particularly obvious for tensile creep data collected at 1875-psi where the strain rate increases significantly. The observed deviation may indicate the existence of a change in creep mechanism at high stress levels, possibly shifting from a process dominated by molecular motions to a damage controlled process. These results demonstrate the successful use of Findley's power law model to evaluate the non-linear, time-dependent creep deformation of this material with accuracies that are generally acceptable for civil engineering applications. Limits on the applicability of this model should be placed at stress levels below 60-percent of the member's capacity; stress levels generally within the range of civil engineering design values.

Evaluation of Linearity: Creep compliance,  $J(t)$ , a measure of the strain per unit of applied stress, is the viscoelastic material property used to describe material behavior during creep loading and can be represented mathematically as:

$$J(t) = \frac{\varepsilon(t)}{\sigma_0} \quad (14)$$

In linearly viscoelastic materials, the creep compliance is independent of stress; a condition that may exist at low stresses. Long-term creep compliance is one performance criteria commonly used to evaluate composite materials (Lin et al., 2004).

Figures 3.5 and 3.6 compare average creep compliance values determined using different stress levels for specimens loaded in compression and tension, respectively.

Creep compliance increases with time and applied stress. Evaluation of the compliance data indicates that this material behaves non-linearly even at stress levels as low as 10-percent of the ultimate stress. Plotting values of compliance (measured 100-minutes following loading) against applied stress shows that for both loading modes, compliance increases linearly with stress (Figure 3.7). Note that the tension compliance increases disproportionately at the 1875-psi stress level, supporting the concept that creep mechanism is changing at higher stress levels. This is consistent with the interpretation of creep models.

Comparing the creep compliance measured in tension and compression, it can be seen that tension produces larger strain values per unit of stress than compression. Assessing the apparent linear relationship between compliance and stress it would appear that tension specimens have 14-percent larger values of compliance at low levels of stress. This finding seems to be justified by static test results where the tensile modulus is 11-percent lower than the compressive modulus (Kobbe, 2005). In addition, the tension specimens tend to accumulate strain 17-percent faster than compression for an equivalent increase in stress.

Figure 3.8 compares the variation of creep rate with applied stress. Examining this figure it is clear that the creep rate is very sensitive to changes in the applied stress. The strain rate increases disproportionately with stress, and strain is accumulated at a greater rate in tension than in compression. This response becomes even more pronounced as stress levels become large.

Comparison of Tension and Compression Creep: Because the static modulus of the WPC is different in tension and compression, it is useful for comparative purposes, to

normalize the creep strains to the initial strain. The relative creep ( $\varepsilon_r = \varepsilon(t)/\varepsilon_0$ ) at 100-minutes is depicted in Figure 3.9. The relative creep increases linearly with applied stress for both tension and compression. The slope of the tension curve is nearly twice that of compression, highlighting the sensitivity of this material to tension loadings that produce time-dependent deflections considerably faster than for compression. At an equivalent stress level, tensile deformations will be significantly larger than compressive deformations.

Contributions of compressive and tensile creep in the time-dependent response of a flexural member are strongly related to the applied stress. As loads intensify, this material exhibits an increasingly pronounced non-linear response at all times. To quantify the relative contributions of compression and tension, a reference stress level approximately equal to the design stresses is used as the basis for comparisons. Research by Haiar (2000) and Slaughter (2004) indicate that design values range from approximately 30 to 40-percent of the ultimate strength of the material. Stress distributions in a full-section flexural member were estimated elsewhere using a moment-curvature analysis and conclude that in bending under design loads, compression and tension have comparable maximum stresses (varying by less than 7-percent) (Kobbe, 2005).

The creep performance evaluated at 100-minutes after load application for loads that approximate design levels is compared in Table 3.4. In a bending member, tension appears to be the most susceptible to long-term performance limitations. While strain and relative creep are similar in compression and tension, creep compliance and strain rate are

significantly higher in tension. Strain is accumulating 26 to 43-percent faster and stiffness is 11 to 17-percent lower in tension.

Time-Stress Superposition: Creep compliance curves over a range of stress levels tend to diverge relatively slowly in log-log plots of compliance versus time. In accordance with the TTSSP analysis discussed previously, horizontal shift factors were employed to produce a single master curve at a reference state of stress for compression and tension compliance data. A Prony series was then fit to each master curve with retardation times ( $\tau_i$ ) taken as  $10^i$  (Figures 3.10 and 3.11). The Prony series coefficients ( $J_0$  and  $J_i$ ) appearing in Equation (13) were determined with a regression analysis using a least squares technique and are listed in Table 3.5.

In order to equate creep compliance in tension and compression, master curves can be evaluated at any single stress level within the range of the data. By shifting the master curve with horizontal shift factors determined from Equation (11) (Figure 3.12), the creep responses in compression and tension were compared at a stress level of 1,000 psi (Figure 3.13). This comparison again illustrates that creep compliance at stresses approximating design conditions are larger and are increasing at a faster rate for tension loads compared to compression.

Master curves generated for compression and tension were proposed as a way to estimate creep compliance many decades of time beyond the test duration. At the lowest stress levels considered, 100-minute creep data in compression was extrapolated to 950,000-minutes (1.81-years) while tension results were estimated to 7,400-minutes (5.14-days). However, when the data was evaluated at design stress levels the

extrapolation was further restricted to a maximum of 390,000 and 734-minutes for compression and tension, respectively.

The ability to project long-term behavior of this material is limited by the magnitude of the ultimate stress in tension. To make predictions on a time scale appropriate for design, longer duration tests are needed. One possible strategy that could expand the master curves to a more useful design life timeframe could include testing over a range of temperatures. It is recognized that these results may not be practical for predicting long-term behavior, but they do confirm the use of time-stress superposition. It should be noted that the non-linear nature of this material makes this procedure subject to scrutiny. There is evidence that this material undergoes changes that are not accounted for by this procedure at stresses above 60-percent of the materials ultimate capacity. While this procedure did not provide for significant acceleration of creep behavior, it was able to further illustrate that fundamental differences exist in the compressive and tensile modes of time-dependent deformation.

### **3.6 Conclusions**

Findley's power law has proven to be an accurate model for creep behavior of this material. Using Findley's stress-independent model, time-dependent strain was predicted with accuracies that are generally acceptable for civil engineering applications. An important restriction to this model is that it cannot describe non-linear tertiary creep; therefore stress levels must be kept sufficiently low. Compressive and tensile creep followed a related power law with similar time exponents. Modeling creep at elevated stress levels resulted in a noticeable amount of divergence, possibly indicating the

existence of another mechanism. This divergence becomes pronounced in compliance at long durations and elevated stresses.

Polypropylene-based WPCs exhibit strong non-linear behavior. Linear behavior of this material seems to exist only at extremely small stresses well below design level. Creep behavior of wood-plastic composites is sensitive to both the mode and magnitude of the applied load. At design level stresses, tensile creep proved to impact long-term performance of a flexural member more so than compressive creep. In particular, strain rates in tension are significantly higher than those found in compression. Improvements in section design and/or tensile reinforcement could have a beneficial effect on the performance of this material.

Creep of this material can be accelerated with increasing stress levels and the use of time-temperature-stress superposition principles to construct a master curve of creep compliance. While it appears that the master curve may have the potential to extend test data by many decades, more long-term creep data is needed in order to further validate the applicability of TTSSP.

### 3.7 References

- Alvarez, V.A., Kenny, J.M., and Vázquez, A., "Creep Behavior of Biocomposites Based on Sisal Fiber Reinforced Cellulose Derivatives/Starch Blends." *Polymer Composites*, Vol. 25, No. 3, pp. 280-288, June 2004.
- ASTM D638-99, "Standard Test Methods for Tensile Properties of Plastics." American Society for Testing and Materials.
- Brinson H.F., Morris, D.H., and Yeow, Y.T., "A New Experimental Method for the Accelerated Characterization of Composite Materials." 6<sup>th</sup> International Conference on Experimental Stress Analysis, Munich, September 18-22, 1978.
- Cessna, L.C., "Stress-Time Superposition of Creep Data for Polypropylene and Coupled Glass-Reinforced Polypropylene." *Polymer Engineering and Science*, Vol. 11, No. 3, pp. 211-219, May 1971.
- Choi, Y. and Yuan, R.L., "Time-Dependent Deformation of Pultruded Fiber Reinforced Polymer Composite Columns." *Journal of Composites for Construction*, Vol. 7, No. 4, pp. 356-362, November 2003.
- Findley, W.N., "Mechanisms and Mechanics of Creep of Plastics." *SPEJ*, Vol. 16, pp. 57-65, January 1960.
- Findley, W.N., Lai, J.S., and Onaran, K., "Creep and Relaxation of Nonlinear Viscoelastic Materials." North-Holland Publishing Company, New York, NY, 1976.
- Findley, W.N., "26-year Creep and Recovery of Polyvinylchloride and Polyethylene." *Polymer Engineering and Science*, Vol. 27, No. 8, pp. 582-585, 1987.
- Flugge, W., "Viscoelasticity." Blaisdell, Waltham, MA, 1967.
- Fung, Y.C., "Foundations of Solid Mechanics." Prentice Hall, Englewood Cliffs, NJ, 1965.
- Haiar, K.J., "Performance and Design of Prototype Wood-Plastic Composite Sections." Master Thesis, Washington State University, May 2000.
- Jazouli, S., Luo, W., Bremand, F., and Vu-Khanh, T., "Application of Time-stress Equivalence to Nonlinear Creep of Polycarbonate." *Polymer Testing*, Vol. 24, pp. 463-467, 2005.
- Knauss, W.G. and Emri, I.J., "Non-Linear Viscoelasticity Based on Free Volume Consideration." *Computers and Structures*, Vol. 13, pp. 123-128, 1981.



- Kobbe, R.G., "Creep Behavior of Wood-Polypropylene Composites." Chapter 2, Master Thesis, Washington State University, June 2005.
- Laver, T.C., "Extruded Synthetic Wood Composition and Method for Making Same." Patent Number 5,516,472. 1996.
- Lai, J. and Bakker, A., "Analysis of the Non-linear Creep of High-Density Polypropylene." *Polymer*, Vol. 36, No. 1, pp. 93-99, 1995.
- Lin, W.S., Pramanick, A.K., and Sain, M., "Determination of Material Constants for Nonlinear Viscoelastic Predictive Model." *Journal of Composite Materials*, Vol. 38, No. 1, pp. 19-29, 2004.
- Lou, Y.C. and Schapery, R.A., "Viscoelastic Characterization of a Nonlinear Fiber-Reinforced Plastic," *Journal of Composite Materials*, Vol. 5, pp. 208-234, 1971.
- Ma, C.C.M, Tai, N.H., Wu, S.H., Lin, S.H., Wu, J.F., and Lin, J.M., "Creep Behavior of Carbon-Fiber-Reinforced Polyetheretherketone (PEEK) Laminated Composites." *Composites Part B*, Vol. 28B, pp. 407-417, 1997.
- Mallick, P.K., "Fiber-Reinforced Composites: Materials, Manufacturing, and Design." Marcel Dekker, New York, NY, 1988.
- Nuñez, A.J., Marcovich, N.E. and Aranguren, M.I., "Analysis of the Creep Behavior of Polypropylene-Woodflour Composites." *Polymer Engineering and Science*, Vol. 44, No. 8, pp. 1594-1603, August 2004.
- Papanicolaou, G.C., Zaoutsos, S.P., and Cardon, A.H., "Further Development of a Data Reduction Method for the Nonlinear Viscoelastic Characterization of FRPs." *Composites Part A*, Vol. 30, pp. 839-848, 1999.
- Park, B. and Balatinecz, J.J., "Short Term Flexural Creep Behavior of Wood-Fiber/Polypropylene Composites." *Polymer Composites*, Vol. 19, No. 4, pp. 377-382, August 1998.
- Park, S.W. and Kim, Y.R., "Fitting Prony-Series Viscoelastic Models with Power-Law Presmoothing." *Journal of Materials in Civil Engineering*, pp. 26-32, January/February 2001.
- Rand, J.L., "A Nonlinear Viscoelastic Creep Model." *Tappi Journal*. Pp. 178-182, July 1995.
- Sain, M.M., Balatinecz, J., and Law, S., "Creep Fatigue in Engineered Wood Fiber and Plastic Compositions." *Journal of Applied Polymer Science*, Vol. 77, pp. 260-268, 2000.

- Schapery, R.A., "On the Characterization of Nonlinear Viscoelastic Materials." *Polymer Engineering and Science*, Vol. 9, No. 4, pp. 295-310, 1969.
- Scott, D.W. and Zureick, A.H., "Compression Creep of a Pultruded E-Glass/Vinylester Composite." *Composites Science and Technology*, Vol. 58, pp. 1361-1369, 1998.
- Shao, Y. and Shanmugam, J., "Deflection Creep of Pultruded Composite Sheet Piling." *Journal of Composites for Construction*, Vol. 8, No. 5, pp. 471-479, October 2004.
- Slaughter, A.E., "Design and Fatigue of a Structural Wood-Plastic Composite." Master Thesis, Washington State University, August 2004.
- Wenbo, L., Ting-Qing, Y, and Qunli, A., "Time-Temperature-Stress Equivalence and its Application to Nonlinear Viscoelastic Materials." *Acta Mechanica Solida Sinica*, Vol. 14, No. 3, pp. 195-199, 2001.
- Wolcott, M.P. and Smith, P.M., "Opportunities and Challenges for Wood-Plastic Composites in Structural Applications." *Proceedings of Progress in Woodfibre-Plastic Composites-2004 Toronto, ON*, 2004.
- Yen, S.C. and Williamson, F.L., "Accelerated Characterization of Creep Response of an Off-Axis Composite Material." *Composite Science and Technology*, Vol. 38, pp. 103-118, 1990.

### 3.8 Tables

**Table 3.1.** Stresses applied in various creep tests

Loading Mode	Stress (psi)	MOR (psi)	Stress Ratio (%)
Compression	4689	7995	58.6%
	3909	7995	48.9%
	3100	7995	38.8%
	2333	7995	29.2%
	1551	7995	19.4%
	777	7995	9.7%
Tension	1875	2906	64.5%
	1599	2906	55.0%
	1436	2906	49.4%
	1150	2906	39.6%
	927	2906	31.9%
	686	2906	23.6%
	466	2906	16.0%
	235	2906	8.1%

**Table 3.2.** Measured strain compared to predictions derived with the general power law.

Loading Mode	Stress (psi)	Creep Parameters <sup>a</sup>				Average Creep Strain (in/in) at Time t (min)					Ave. Error
		$\epsilon_0$ (in/in)	m ( $\epsilon$ )	n	$r^2$	t = 1	t = 30	t = 60	t = 90		
Compression	Predictions using General Power Law										
	4689	1.06E-02	1.49E-03	0.278	0.972	1.37E-02	1.87E-02	2.04E-02	2.16E-02	0.53%	
	3909	8.36E-03	1.04E-03	0.272	0.971	1.05E-02	1.39E-02	1.50E-02	1.58E-02	0.51%	
	3100	6.50E-03	6.54E-04	0.277	0.966	7.89E-03	1.01E-02	1.08E-02	1.13E-02	0.52%	
	2333	4.44E-03	3.10E-04	0.289	0.974	5.12E-03	6.25E-03	6.66E-03	6.93E-03	0.35%	
	1551	2.74E-03	1.39E-04	0.293	0.969	3.05E-03	3.57E-03	3.76E-03	3.89E-03	0.36%	
	777	1.28E-03	5.51E-05	0.274	0.961	1.39E-03	1.57E-03	1.63E-03	1.67E-03	0.39%	
	Experimental Measurements										
	4689	-----	-----	-----	-----	1.35E-02	1.88E-02	2.04E-02	2.13E-02	-----	
	3909	-----	-----	-----	-----	1.04E-02	1.40E-02	1.50E-02	1.56E-02	-----	
	3100	-----	-----	-----	-----	7.78E-03	1.01E-02	1.08E-02	1.12E-02	-----	
	2333	-----	-----	-----	-----	5.08E-03	6.29E-03	6.64E-03	6.87E-03	-----	
	1551	-----	-----	-----	-----	3.02E-03	3.59E-03	3.75E-03	3.86E-03	-----	
	777	-----	-----	-----	-----	1.38E-03	1.58E-03	1.63E-03	1.66E-03	-----	
Tension	Predictions using General Power Law										
	1875	3.90E-03	2.86E-04	0.336	0.985	4.61E-03	6.13E-03	6.71E-03	7.12E-03	0.35%	
	1599	3.01E-03	2.04E-04	0.314	0.979	3.49E-03	4.39E-03	4.73E-03	4.96E-03	0.32%	
	1436	2.71E-03	1.60E-04	0.310	0.974	3.08E-03	3.77E-03	4.02E-03	4.20E-03	0.27%	
	1150	2.17E-03	1.34E-04	0.271	0.978	2.45E-03	2.87E-03	3.02E-03	3.12E-03	-0.07%	
	927	1.65E-03	7.56E-05	0.286	0.957	1.82E-03	2.09E-03	2.18E-03	2.25E-03	-0.44%	
	686	1.25E-03	4.38E-05	0.287	0.935	1.35E-03	1.51E-03	1.56E-03	1.60E-03	0.38%	
	466	8.19E-04	3.43E-05	0.258	0.928	8.88E-04	9.85E-04	1.02E-03	1.04E-03	-0.44%	
	235	4.00E-04	7.04E-06	0.338	0.631	4.18E-04	4.56E-04	4.71E-04	4.81E-04	-0.07%	
	Experimental Measurements										
	1875	-----	-----	-----	-----	4.58E-03	6.14E-03	6.69E-03	7.08E-03	-----	
	1599	-----	-----	-----	-----	3.47E-03	4.42E-03	4.71E-03	4.93E-03	-----	
	1436	-----	-----	-----	-----	3.06E-03	3.78E-03	4.02E-03	4.17E-03	-----	
	1150	-----	-----	-----	-----	2.45E-03	2.87E-03	3.03E-03	3.11E-03	-----	
927	-----	-----	-----	-----	1.84E-03	2.11E-03	2.17E-03	2.26E-03	-----		
686	-----	-----	-----	-----	1.34E-03	1.49E-03	1.57E-03	1.59E-03	-----		
466	-----	-----	-----	-----	8.88E-04	9.95E-04	1.02E-03	1.04E-03	-----		
235	-----	-----	-----	-----	4.11E-04	4.49E-04	4.73E-04	4.97E-04	-----		

<sup>a</sup> Average of 8 results.

**Table 3.3.** Measured strain compared to predictions derived with Findley's power law.

Loading Mode	Stress (psi)	Creep Parameters <sup>a</sup>			n	Average Creep Strain (in/in) at Time t (min)					Ave. Error
		$\epsilon_0$ (in/in)	$\epsilon_0'$	$m'(\epsilon)$		t=1	t=30	t=60	t=90		
Compression	Predictions using Findley's Non-Linear Model										
	4689	1.06E-02	7.48E-03	2.10E-04	0.281	1.39E-02	1.91E-02	2.09E-02	2.22E-02	2.73%	
	3909	8.36E-03	7.48E-03	2.10E-04	0.281	1.04E-02	1.37E-02	1.49E-02	1.57E-02	-0.48%	
	3100	6.50E-03	7.48E-03	2.10E-04	0.281	7.54E-03	9.59E-03	1.03E-02	1.08E-02	-4.12%	
	2333	4.44E-03	7.48E-03	2.10E-04	0.281	5.31E-03	6.58E-03	7.02E-03	7.32E-03	5.40%	
	1551	2.74E-03	7.48E-03	2.10E-04	0.281	3.37E-03	4.09E-03	4.35E-03	4.52E-03	14.55%	
	777	1.28E-03	7.48E-03	2.10E-04	0.281	1.64E-03	1.97E-03	2.09E-03	2.16E-03	25.72%	
	Experimental Measurements										
	4689	-----	-----	-----	-----	1.35E-02	1.88E-02	2.04E-02	2.13E-02	-----	
	3909	-----	-----	-----	-----	1.04E-02	1.40E-02	1.50E-02	1.56E-02	-----	
3100	-----	-----	-----	-----	7.78E-03	1.01E-02	1.08E-02	1.12E-02	-----		
2333	-----	-----	-----	-----	5.08E-03	6.29E-03	6.64E-03	6.87E-03	-----		
1551	-----	-----	-----	-----	3.02E-03	3.59E-03	3.75E-03	3.86E-03	-----		
777	-----	-----	-----	-----	1.38E-03	1.58E-03	1.63E-03	1.66E-03	-----		
Tension	Predictions using Findley's Non-Linear Model										
	1875	3.90E-03	3.08E-03	5.93E-05	0.300	4.48E-03	5.63E-03	6.05E-03	6.33E-03	-7.65%	
	1599	3.01E-03	3.08E-03	5.93E-05	0.300	3.58E-03	4.39E-03	4.68E-03	4.89E-03	0.34%	
	1436	2.71E-03	3.08E-03	5.93E-05	0.300	3.11E-03	3.77E-03	4.00E-03	4.17E-03	0.16%	
	1150	2.17E-03	3.08E-03	5.93E-05	0.300	2.36E-03	2.82E-03	2.98E-03	3.09E-03	-1.98%	
	927	1.65E-03	3.08E-03	5.93E-05	0.300	1.85E-03	2.17E-03	2.29E-03	2.37E-03	3.59%	
	686	1.25E-03	3.08E-03	5.93E-05	0.300	1.33E-03	1.55E-03	1.63E-03	1.69E-03	3.40%	
	466	8.19E-04	3.08E-03	5.93E-05	0.300	8.89E-04	1.03E-03	1.08E-03	1.12E-03	4.22%	
	235	4.00E-04	3.08E-03	5.93E-05	0.300	4.43E-04	5.12E-04	5.37E-04	5.54E-04	11.81%	
	Experimental Measurements										
1875	-----	-----	-----	-----	4.58E-03	6.14E-03	6.69E-03	7.08E-03	-----		
1599	-----	-----	-----	-----	3.47E-03	4.42E-03	4.71E-03	4.93E-03	-----		
1436	-----	-----	-----	-----	3.06E-03	3.78E-03	4.02E-03	4.17E-03	-----		
1150	-----	-----	-----	-----	2.45E-03	2.87E-03	3.03E-03	3.11E-03	-----		
927	-----	-----	-----	-----	1.84E-03	2.11E-03	2.17E-03	2.26E-03	-----		
686	-----	-----	-----	-----	1.34E-03	1.49E-03	1.57E-03	1.59E-03	-----		
466	-----	-----	-----	-----	8.88E-04	9.95E-04	1.02E-03	1.04E-03	-----		
235	-----	-----	-----	-----	4.11E-04	4.49E-04	4.73E-04	4.97E-04	-----		

<sup>a</sup> Average of 8 results.

**Table 3.4.** Creep performance at design level stress evaluated 100-min after loading.

	Stress (psi)	Strain (in/in)	Strain Rate (min <sup>-1</sup> )	Compliance (1/psi)	Relative Creep
<b>Compression</b>	1,000	2.31E-03	2.01E-06	2.272E-06	1.2948
<b>Tension</b>	1,000	2.16E-03	2.70E-06	2.541E-06	1.3295
% difference	--	-6.6%	25.5%	10.6%	2.6%
<b>Compression</b>	1,500	3.54E-03	3.88E-06	2.507E-06	1.3657
<b>Tension</b>	1,500	3.59E-03	6.82E-06	3.032E-06	1.5212
% difference	--	1.4%	43.2%	17.3%	10.2%

**Table 3.5.** Coefficients used in the Prony series.

i	Compression		Tension	
	J <sub>i</sub> (psi <sup>-1</sup> )	τ <sub>i</sub> (min)	J <sub>i</sub> (psi <sup>-1</sup> )	τ <sub>i</sub> (min)
<b>0</b>	1.687E-06	∞	1.806E-06	∞
<b>1</b>	1.084E-07	10	1.240E-07	10
<b>2</b>	1.736E-07	10 <sup>2</sup>	1.243E-07	10 <sup>2</sup>
<b>3</b>	2.268E-07	10 <sup>3</sup>	2.350E-07	10 <sup>3</sup>
<b>4</b>	3.412E-07	10 <sup>4</sup>	3.318E-07	10 <sup>4</sup>
<b>5</b>	5.139E-07	10 <sup>5</sup>	9.503E-07	10 <sup>5</sup>
<b>6</b>	6.291E-07	10 <sup>6</sup>	--	--
<b>7</b>	1.517E-06	10 <sup>7</sup>	--	--

### 3.9 Figures

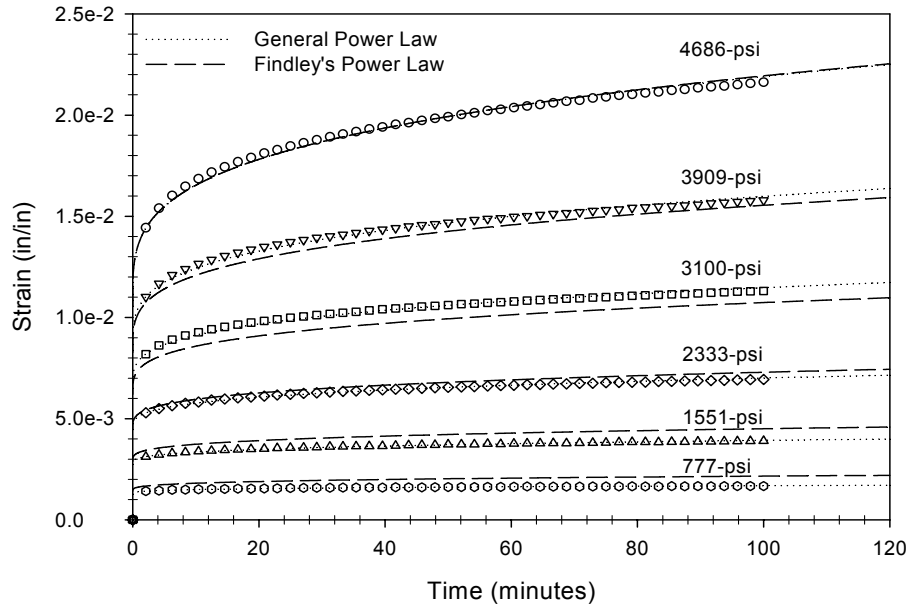


**Fig. 3.1.** Measurements and predictions for creep strain in compression.

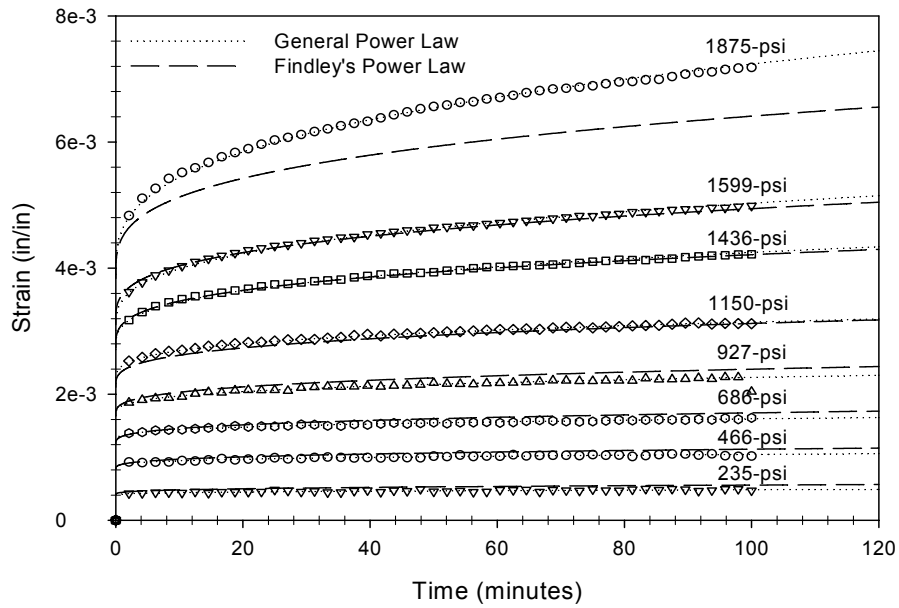


**Fig. 3.2.** Measurements and predictions for creep strain in tension.

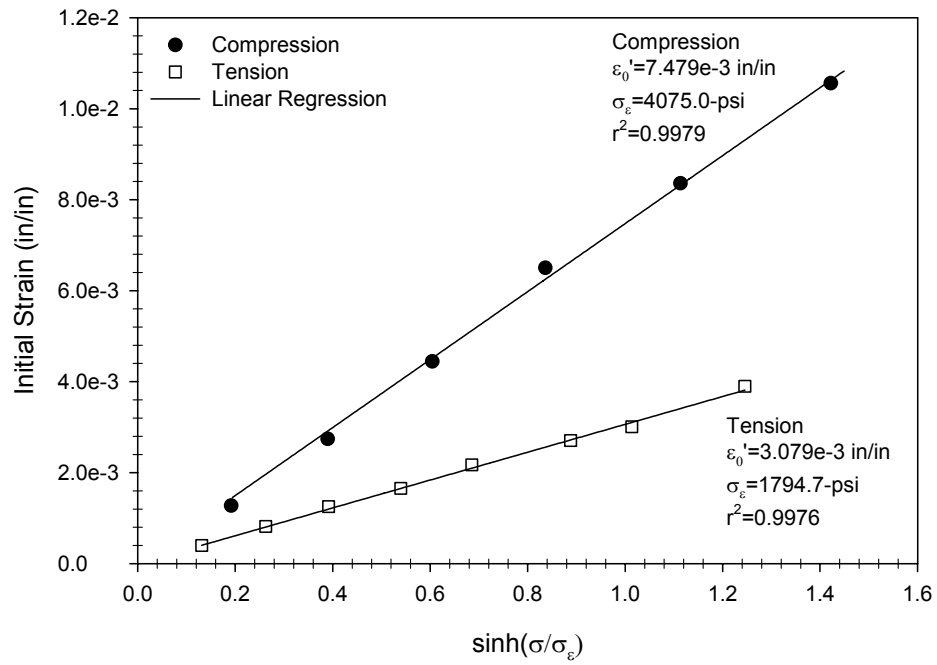


**Fig. 3.3.** Evaluation of the creep parameters  $\epsilon_0'$  and  $\sigma_\epsilon$ .

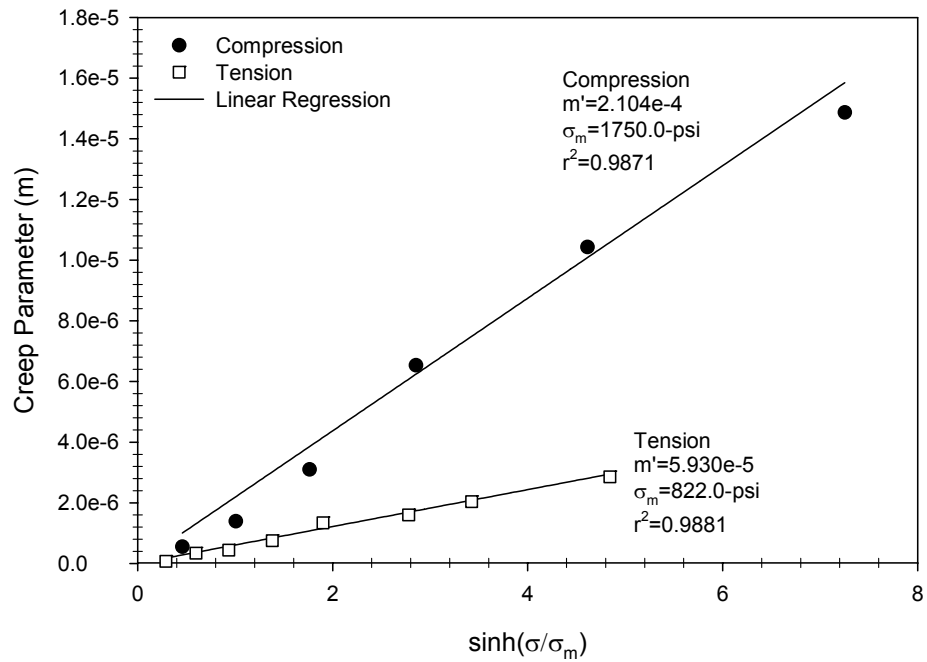


**Fig. 3.4.** Evaluation of the creep parameters  $m'$  and  $\sigma_m$ .



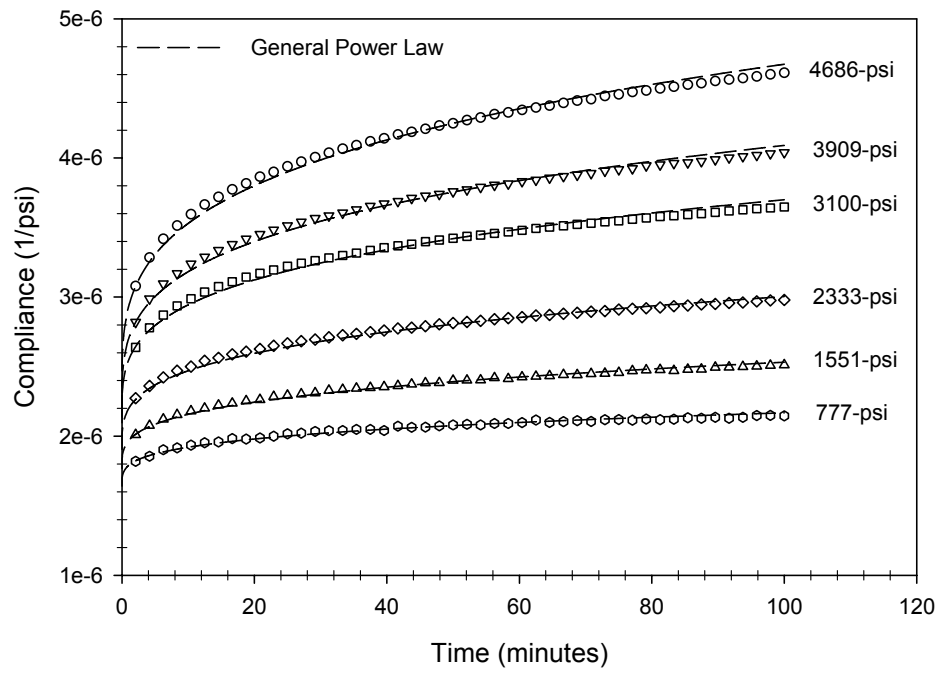


**Fig. 3.5.** Creep compliance measurements for compression.

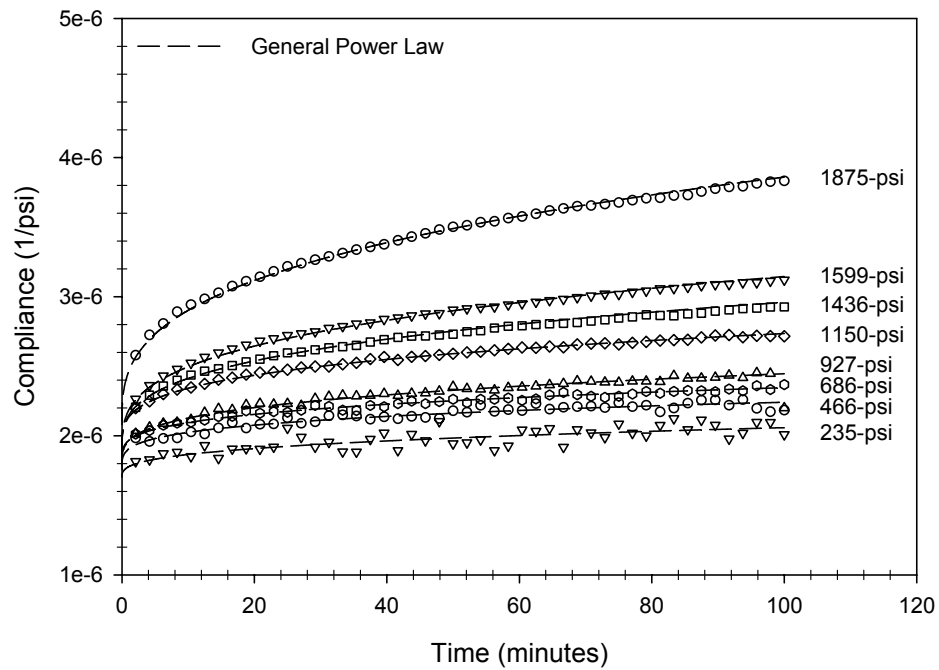


**Fig. 3.6.** Creep compliance measurements for tension.

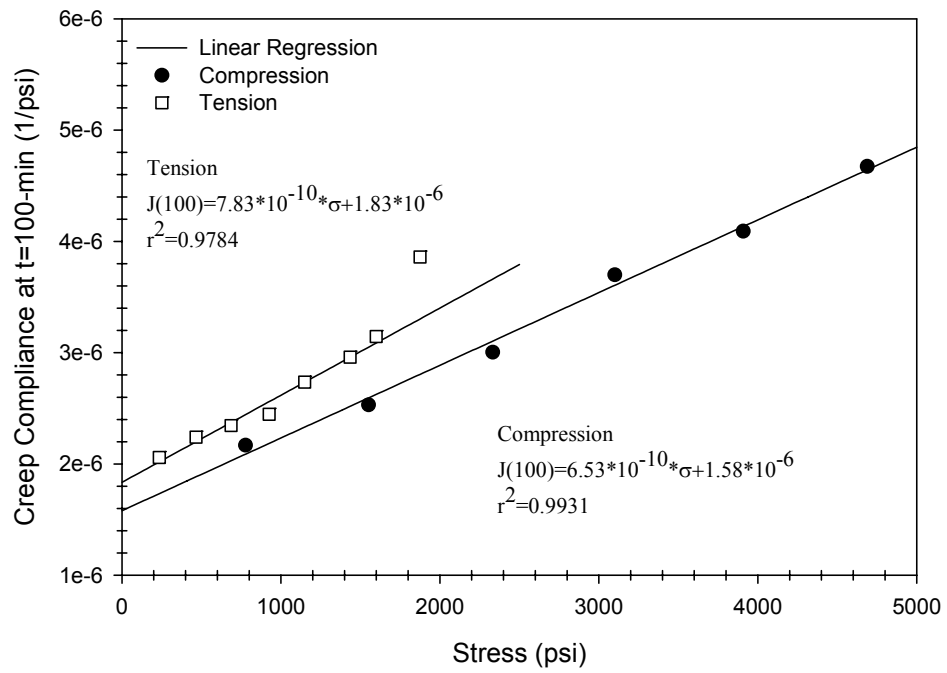


**Fig. 3.7.** Creep compliance as a function of applied stress.

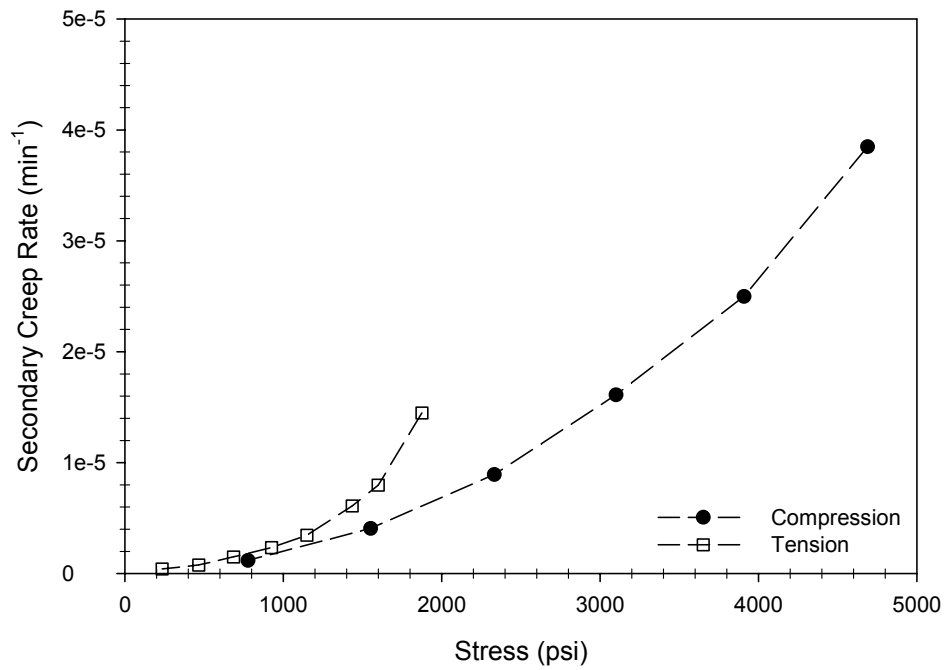


**Fig. 3.8.** Creep rate as a function of applied stress.

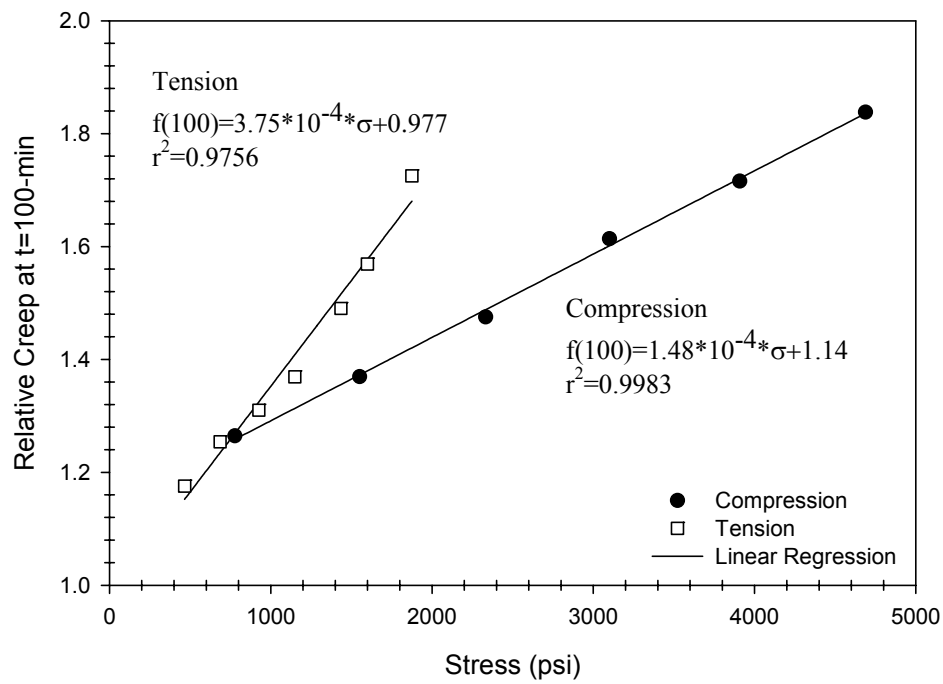


**Fig. 3.9.** Relative creep as a function of applied stress.

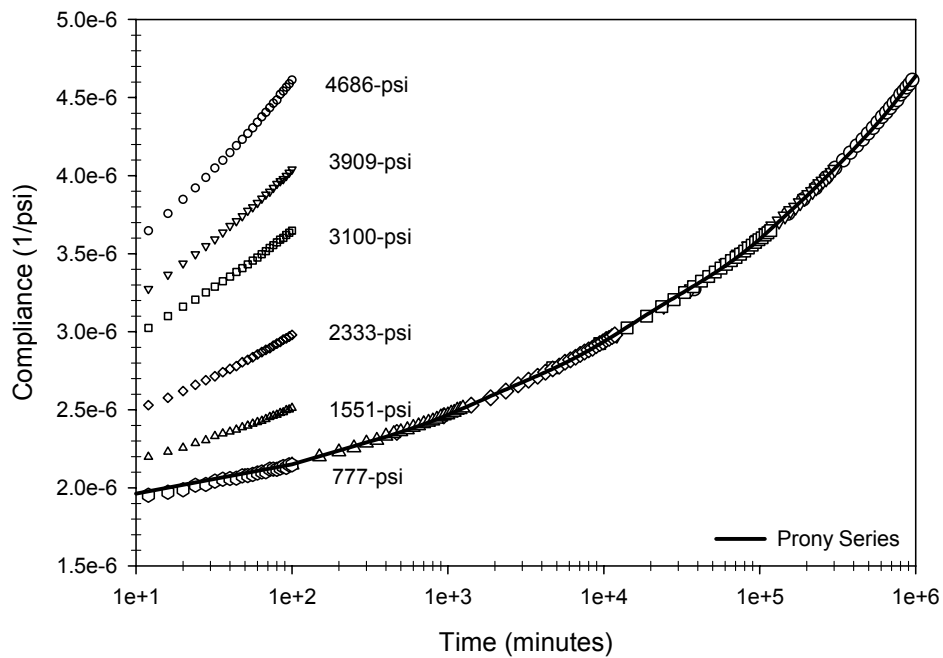


**Fig. 3.10.** The master curve for the creep compliance at 777 psi in compression. (Coefficients used in the Prony series can be found in Table 2.5)

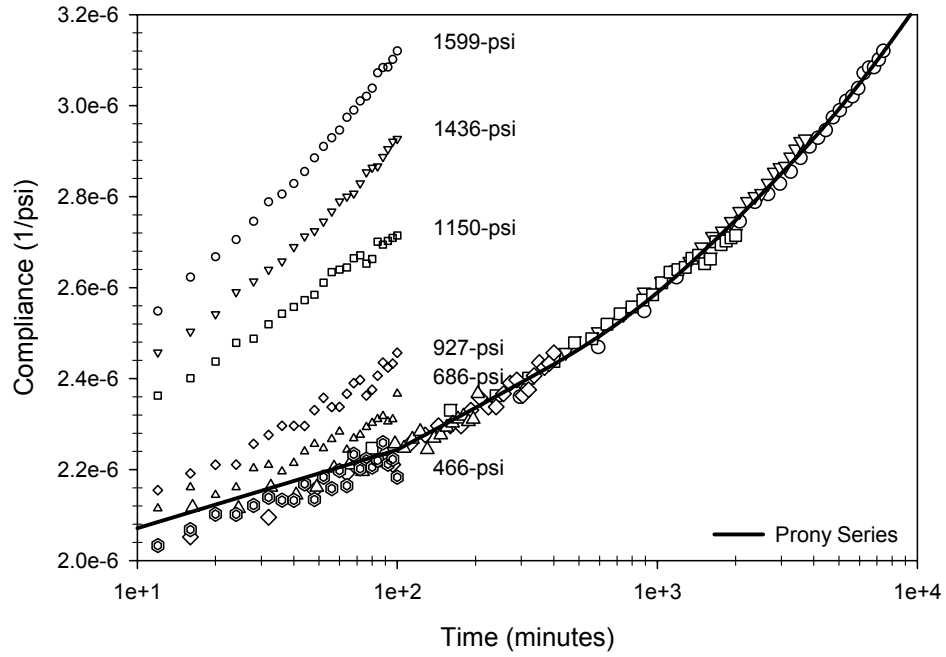


**Fig. 3.11.** The master curve for the creep compliance at 466 psi in tension. (Coefficients used in the Prony series can be found in Table 2.5)

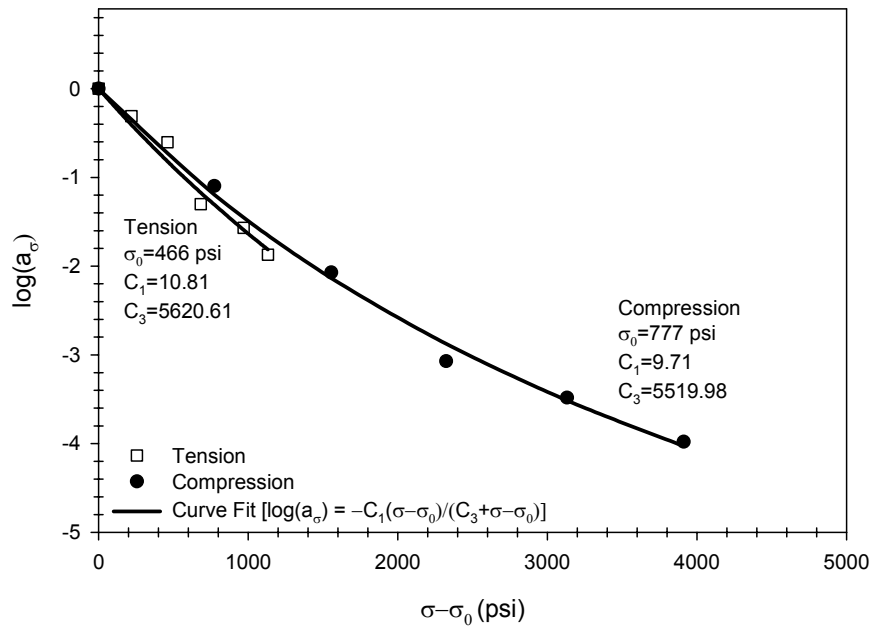


**Fig. 3.12.** Variation of stress shift factor with stress difference for compression and tension.

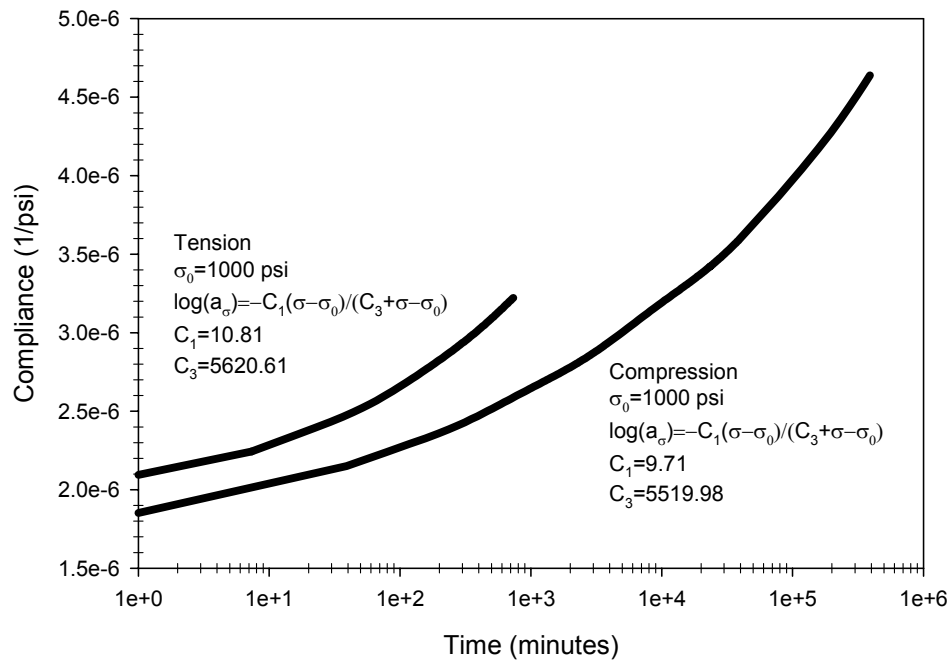


**Fig. 3.13.** Compliance master curves for compression and tension at 1000 psi.

## **APPENDIX A – DOWEL BEARING TESTING**

### **A.1 Introduction**

As the wood-plastic composite (WPC) market continues to grow, the use of these materials in structural applications is becoming more common. In the design of structural members, connection strength is an essential consideration. Very little data is currently available pertaining to the connection performance of WPCs. This work is intended to provide insight into the dowel bearing performance of a polypropylene-based WPC.

### **A.2 Materials and Methods**

The material investigated was a polypropylene wood-plastic composite. Solid deck board specimens (1-in. (2.54-cm) by 5.5-in. (13.97-cm)) were produced using a conical counter-rotating twin-screw extruder. All specimens were composed of a polypropylene (PP) based formulation consisting of 58.8-percent pine (*Pinus* spp.) flour (60-mesh, Amercian Wood Fibers 6020), 33.8-percent polypropylene (PP) matrix resin (Solvay HB9200), 4-percent talc (Luzenac Nicron 403), 2.3-percent maleic anhydride polypropylene (MAPP) coupling agent (Honeywell 950P), and 1.0-percent lubricant (Honeywell OP100) by weight. Specimens were machined to size and environmentally conditioned at 70° F (21.1° C) and 50-percent RH. Testing was performed in an environmentally conditioned room controlled to 70° F (21.1° C) and 50-percent RH.

Dowel bearing strength was evaluated following ASTM D5764. Four test groups, chosen to investigate the dowel bearing strength of ½-in. (12.7-mm) and ¼-in. (6.4-mm)

diameter bolts as well as 16d-common (0.164-in. (4.2-mm)) and 16d-box (0.131-in. (3.3-mm)) nails, were cut from a solid deck board section (nominally 1-inch (25.4-mm) thick) to the final dimensions of 2-inches (50.8-mm) wide and 2-inches (50.8-mm) high. For bolts, the hole size was 1/16-in. (1.6-mm) larger than the bolt diameter. ASTM D5764 recommends that driven fasteners be inserted in holes that are smaller than the diameter and then removed before sawing through the hole to produce a half-hole specimen. However, for this material even pre-drilled holes with the allowable pilot diameter, resulted in nails splitting the specimen when driven. For nail tests, it was found that a pilot hole of equal size to the fastener diameter was needed to prevent splitting and ensure that once driven, the fastener could be removed without damage to the specimen. Tests were conducted at a displacement rate of 0.04-in/min (1.0-mm/min). A 30-kip universal electromechanical test machine (Instron 4400R) was utilized for load application and data was acquired in real time by computer at 5 Hz.

### **A.3 Results and Discussion**

The average dowel-bearing strengths for ½-in. and ¼-in. bolts as well as 16d-common and 16d-box nails were found to be 12.7, 16.3, 19.0, and 20.5-ksi (87.4, 112.3, 131.2, and 141.5-MPa), respectively (Table A.1). The associated coefficients of variation (COV) were 1.75, 1.87, 2.36, and 2.60-percent. Testing conducted by Balma (1999) on similar solid sections found dowel-bearing strengths, for ½-inch bolts, to be 3.39 and 5.18-ksi for LDPE and HDPE, respectively. In similar work conducted on hollow specimens, Parsons (2001) reported values of 4.68 to 6.31-ksi for HDPE and 16.8 to 20.1-ksi for PVC. The dowel bearing strength of this material appears to be significantly

greater than that found for LDPE and HDPE and compares well with that of PVC. The failure mode exhibited by this formulation was out-of-plane ductile deformation similar to HDPE as opposed to the brittle failures reported for PVC (Parsons, 2001).

#### **A.4 Conclusions**

Experimental results presented, help establish the dowel bearing strength for a polypropylene-based wood-plastic composite. Overall, this material offers a good balance of strength and ductility. Consistent with previous studies, dowel-bearing strength is increased by decreasing the dowel diameter, and will need to be considered in the design of WPC connections (Parsons, 2001).



## **A.5 References**

- ASTM D5764-97a, "Standard Test Methods for Evaluating Dowel-Bearing Strength of Wood and Wood-Based Products." American Society for Testing and Materials.
- Balma, D.A., "Evaluation of Bolted Connections on Wood Plastic Composites." Master Thesis, Washington State University, December, 1999.
- Parsons, W.R., "Energy-Based Modeling of Dowel-Type Connections in Wood-Plastic Composite Hollow Sections." Master Thesis, Washington State University, 2001.

## A.6 Tables

**Table A.1.** Dowel-bearing strength data for a PP-based formulation.

<b>Fastener</b>	<b>Sample Size</b>	<b>Max Load (lbf)</b>	<b>COV (%)</b>	<b>Ave. Bearing Strength (ksi)</b>	<b>COV (%)</b>
1/2" bolt	36	5826	1.77%	12.7	1.75%
1/4" bolt	35	3979	1.62%	16.3	1.87%
16d common nail	32	3174	2.74%	19.0	2.36%
16d box nail	31	2882	2.45%	20.5	2.60%

## **APPENDIX B – COUPON FLEXURE STATIC TESTING**

### **B.1 Introduction**

Driven by ever increasing demand from the commercial construction industry, wood-plastic composites (WPCs) have an established market presence. While WPC development has grown steadily to meet consumer demand, there is a continued need to establish relevant mechanical properties. This work is intended to provide additional insight into the mechanical performance and characterization of a polypropylene-based WPC.

### **B.2 Analytical Methods**

The analytical methods followed in this work are the same as those used in Kobbe (2005); following is a brief summary of that discussion. WPCs, like many other engineering materials, exhibit non-linear stress behavior and properties that are dependent on the loading mode (Altenbach, 2002; Bengtsson, 2000). Knowledge and characterization of mechanical behavior typically requires the use of mathematical models. The accuracy of these models is crucial for structural design. Non-linear constitutive relations in conjunction with section dimensions can be employed in a moment-curvature analysis to determine the load-deformation behavior of an arbitrary section. The information provided from moment-curvature analysis can account for stress contributions from different compression and tension behavior and provide insight that may facilitate improvements in section design.

### B.3 Materials and Methods

All specimens were composed of a polypropylene (PP) based formulation consisting of 58.8-percent pine (*Pinus* spp.) flour (60-mesh, Amercian Wood Fibers 6020), 33.8-percent polypropylene (PP) matrix resin (Solvay HB9200), 4-percent talc (Luzenac Nicron 403), 2.3-percent maleic anhydride polypropylene (MAPP) coupling agent (Honeywell 950P), and 1.0-percent lubricant (Honeywell OP100) by weight. Triple box, hollow sections were extruded with an 86-mm conical twin-screw extruder using a stranding die (Laver, 1996). The extruded profile has a nominal wall thickness of 0.4-in. (1.02-cm) and nominal outside dimensions of 1.8-in. (5-cm) depth and 6.5-in. (17-cm) width. Specimens were machined to size and environmentally conditioned at 70° F (21.1° C) and 50-percent RH. Testing was performed in an environmentally conditioned room controlled to 70° F (21.1° C) and 50-percent RH.

Coupon flexural properties were established following ASTM D790. Specimens were cut from the flange of a standard triple box section and machined to a uniform thickness. Weak axis simple bending tests were carried out on specimens with dimensions that were: 1.18-in. (30-mm) wide, 0.35-in. (8.8-mm) deep, and 6.89-in. (175-mm) long. All tests were conducted at a strain rate of 0.01 (in/in)/min ((mm/mm)/min) which corresponded to a crosshead deflection rate of 0.157-in/min (3.98-mm/min). A 2- kip universal electromechanical test machine (Instron 4466R) was utilized for load application and, data was acquired in real time by computer at 2 Hz. Calculations performed include strain at failure, modulus of elasticity (MOE), and modulus of rupture (MOR).

#### **B.4 Results and Discussion**

The stress-strain curve shown in Figure B.1 indicated that the proportionality limit for coupon flexure data was between 10 and 20-percent of the ultimate stress and, this range was used as a reference to determine the modulus of elasticity. The final two columns found in Table B.1 show the average MOR and MOE to be 4,826 and 527,125-psi (33.27 and 3634.40-Mpa), respectively. Strain at failure was found to be 1.32-in/in (mm/mm). Mechanical property coefficients of variation among specimens were found to range from 5 to 6-percent.

The Moment-curvature analysis, conducted with a program developed by Haiar (2000), was able to capture the general shape of the load-displacement curve. However, experimentally obtained values for maximum load and deflection respectively were 14 and 29-percent larger than moment-curvature predictions, as can be seen in Figure B.2. This deviation, shown in Table B.2, was significantly larger than that found in full-section testing (Kobbe, 2005). This discrepancy was also reported by Haiar (2000) in his work, and it was speculated that size, shape, and/or production effects were the possible causes for the observed differences. Law (1982) also reported calculated bending values falling below experimental observations and he noted that strain on the tensile face at maximum bending load is often higher than failure strains found in direct tension. He surmised that some of this increase is attributable to the presence of material strength distribution, and he observed that when size effects were included, MOR was predicted with increased accuracy. Additionally, Laws (1982) proposed an analysis technique that accounts for the distribution of flaws on the bending strength of non-linear materials.

Other possible explanations for these differences include: redistribution of energy within the section; the impact of scale on energy redistribution; removal of dense surface material in coupon specimens; and relief of processing stresses during machining. Nevertheless, no single cause appears to fully describe the differences observed in coupon and full-section strength predictions.

Compressive and tensile stresses will not be distributed uniformly in this non-linear material. It can be seen in Figure B.3 that as the ultimate load is reached, compressive stress is dominant. Compressive stress at failure was found to be 26-percent greater than tensile stress at failure. At stress levels between 30 and 40-percent of the material's ultimate strength, stress in compression is 9 to 12-percent greater than that in tension. The differences between full-scale and coupon stress distribution is most likely the result of many factors including geometric differences, test configuration, and material preparation.

Due to the magnitude of the strength differences exhibited in compression and tension, it is anticipated that the neutral axis will migrate upwards as a result of lower tensile capacity as moment increases. Figure B.4 shows the neutral axis location as a function of applied load. As the applied moment increases, equilibrium is maintained by the neutral axis shifting away from the tension face.

## **B.5 Conclusions**

Experimental results presented help to establish stress-strain relations and material properties for a polypropylene-based wood-plastic composite. The use of moment-curvature analysis was found to predict the general shape of the load-

displacement response with reasonable accuracy. However, differences between full-section and coupon predictions were noted.

## B.6 References

- Altenbach, H., "Creep Analysis of Thin-Walled Structures." *Z. Angew. Math. Mech.*, Vol. 82, No. 8, pp. 507-533, 2002.
- ASTM D790-99, "Standard Test Methods for Flexural Properties of Unreinforced and Reinforced Plastics and Electrical Insulating Materials." American Society for Testing and Materials.
- Bengtsson, C., "Creep of Timber in Different Loading Modes—Material Property Aspects." World Conference on Timber Engineering, Whistler Resort, British Columbia, Canada, July 31 – August 3, 2000.
- Haiar, K.J., "Performance and Design of Prototype Wood-Plastic Composite Sections." Master Thesis, Washington State University, May 2000.
- Kobbe, R.G., "Creep Behavior of Wood-Polypropylene Composites." Chapter 2, Master Thesis, Washington State University, June 2005.
- Laver, T.C., "Extruded Synthetic Wood Composition and Method for Making Same." Patent Number 5,516,472. 1996.
- Laws, V., "The Relationship Between Tensile and Bending Properties of Non-linear Composite Materials." *Journal of Materials Science*, Vol. 17, pp. 2919-2924, 1982.



## B.7 Tables

**Table B.1.** Coupon flexure mechanical properties.

<b>Specimen</b>	<b>Max Load</b>	<b>Max Deflection</b>	<b>Stain at Failure</b>	<b>MOR</b>	<b>MOE</b>
	<b>(lbf)</b>	<b>(in)</b>	<b>(%)</b>	<b>(psi)</b>	<b>(psi)</b>
1	77.1	0.1930	1.23%	4,643	530,052
2	85.4	0.2430	1.53%	5,281	515,980
3	91.0	0.2080	1.33%	5,456	569,006
4	76.6	0.2080	1.32%	4,651	524,090
5	84.6	0.2150	1.37%	5,096	540,254
6	79.1	0.2030	1.28%	4,833	509,044
7	84.5	0.2060	1.31%	5,133	541,100
8	85.9	0.2170	1.38%	5,210	572,434
9	77.5	0.2050	1.31%	4,656	536,075
10	78.6	0.2180	1.38%	4,756	510,021
11	80.2	0.1920	1.22%	4,823	575,229
12	86.4	0.2070	1.33%	5,115	565,646
13	79.4	0.2190	1.41%	4,698	512,690
14	75.9	0.1970	1.27%	4,473	514,125
15	79.4	0.1990	1.27%	4,713	496,079
16	72.4	0.1930	1.23%	4,317	517,749
17	81.7	0.2160	1.36%	4,993	543,389
18	84.5	0.2140	1.38%	4,958	560,220
19	81.0	0.2060	1.30%	4,913	553,075
20	79.6	0.1880	1.19%	4,817	537,361
21	85.2	0.2190	1.39%	5,180	548,123
22	75.6	0.2060	1.31%	4,519	483,636
23	85.7	0.2140	1.36%	5,189	518,231
24	76.0	0.1940	1.23%	4,632	523,706
25	76.9	0.2200	1.40%	4,633	492,699
26	78.1	0.2030	1.30%	4,667	494,558
27	71.4	0.2070	1.32%	4,302	489,363
28	74.8	0.2030	1.29%	4,476	485,563
<b>Average</b>	80.2	0.2076	1.32%	4,826	527,125
<b>COV (%)</b>	5.91%	5.54%	5.39%	6.19%	5.19%

**Table B.2.** Measured loads compared to predictions found with moment-curvature analysis.

	Deflection (in)	Measured Load <sup>a</sup> (lbs)	Predicted Load <sup>b</sup> (lbs)	% Difference
Coupon Flexure	0.0125	5	8	74%
	0.0250	11	16	40%
	0.0375	18	23	29%
	0.0500	25	30	22%
	0.0625	31	37	17%
	0.0750	37	43	14%
	0.0875	43	48	11%
	0.1000	49	53	9%
	0.1125	54	58	7%
	0.1250	59	62	6%
	0.1375	63	66	5%
	0.1500	67	69	3%
	Average Error			20%

<sup>a</sup> Average of static test results

<sup>b</sup> Moment Curvature Analysis

## B.8 Figures

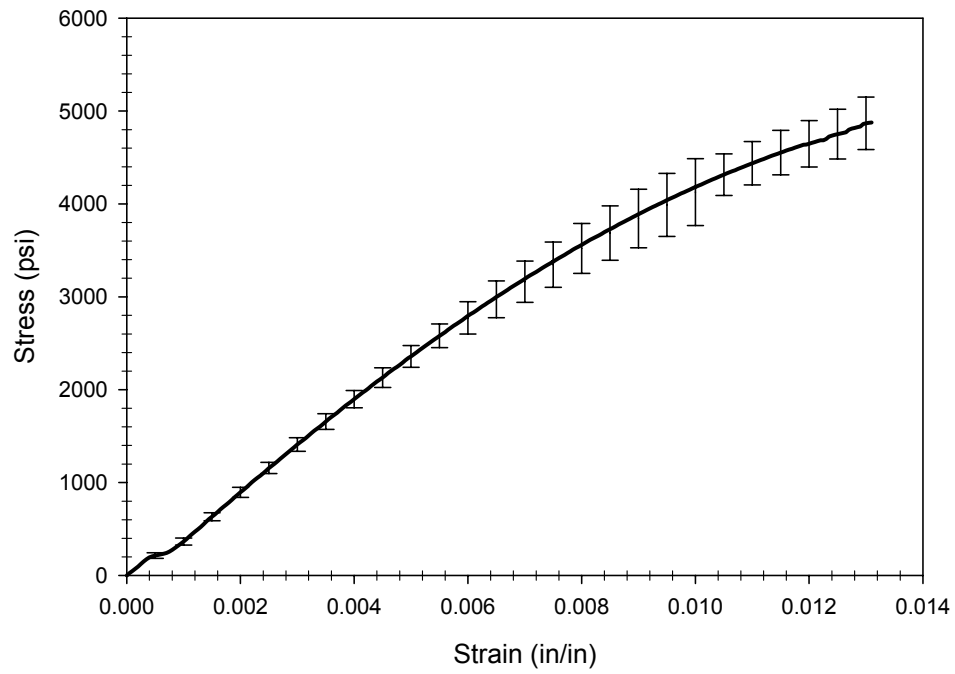


**Fig. B.1.** Coupon flexure stress-strain curves.  
(error bars represent one standard deviation)

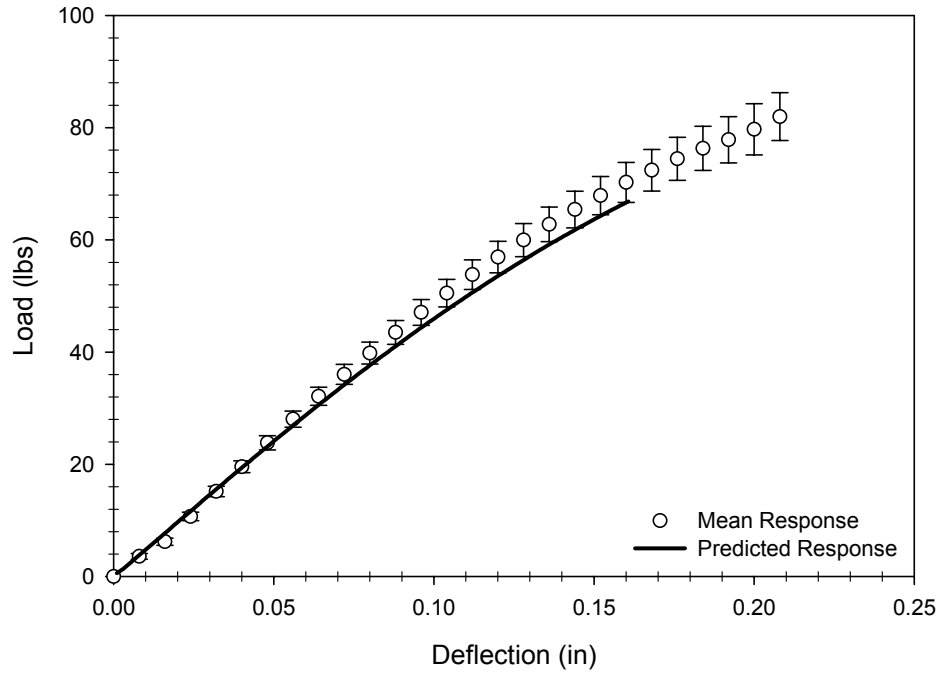


**Fig. B.2.** Measured load-displacement curves compared with moment-curvature predictions (coupon flexure).

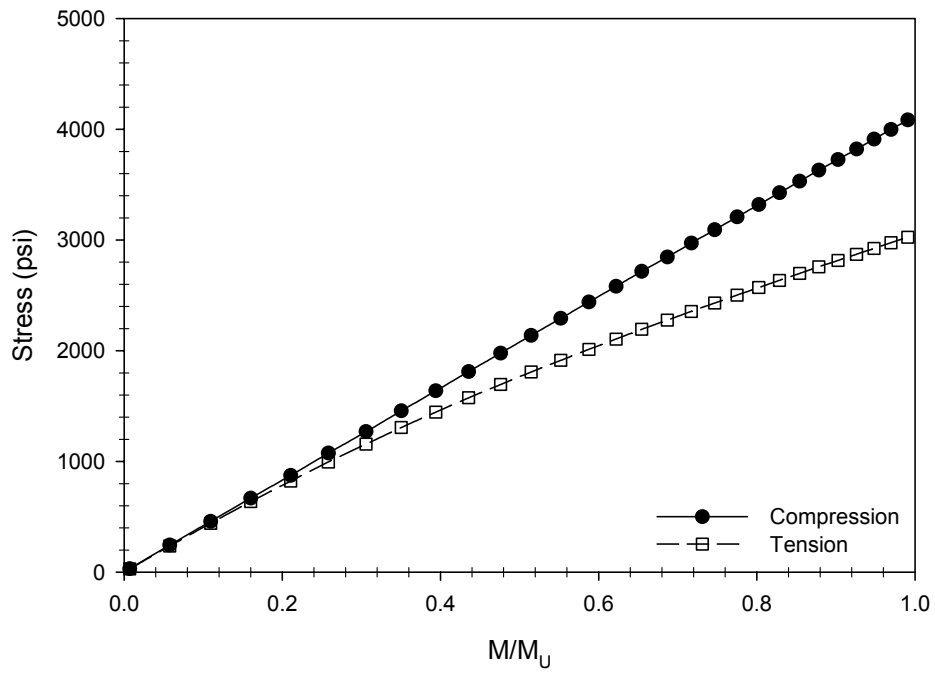


**Fig. B.3.** Predicted compressive and tensile outer fiber stress as a function of applied moment (coupon flexure).

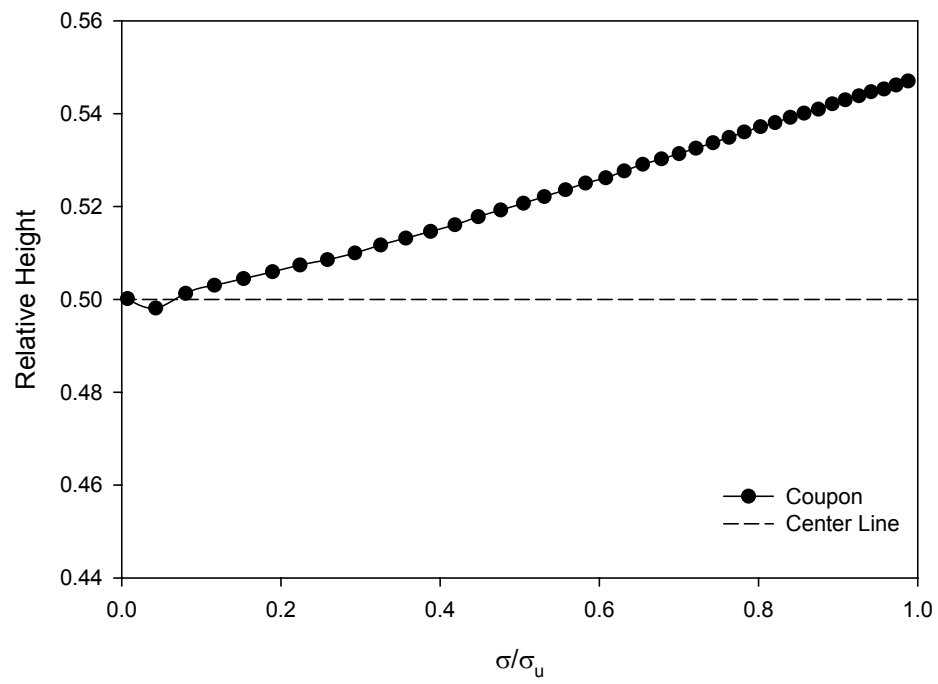


**Fig. B.4.** Location of the neutral axis as a function of applied stress.

## **APPENDIX C – FLEXURE CREEP TESTING**

### **C.1 Introduction**

The wide spread use of wood plastic composites in engineering applications requires sufficient material property knowledge and predictive capability. Most polymer-based composites exhibit time dependent mechanical behavior, typically referred to as viscoelasticity (Jazouli, 2005). Theories available to predict linear viscoelasticity are well advanced and capable of predicting creep behavior of linear materials with remarkable accuracy (Findley et al., 1976; Findley, 1960; Fung, 1965; Flugge, 1967). Non-linear viscoelastic theories continue to be the subject of considerable research and are hampered by a lack of experimental results (Findley, 1960; Lou and Schapery, 1971; Rand, J.L., 1995; Schapery, 1969). The goal of this research is to identify the range of this material's linear viscoelastic response and propose an appropriate model from which generalizations on time-dependent responses can be based.

### **C.2 Analytical Methods**

A reliable and widely recognized creep model was used to evaluate the time-dependent deformation of WPCs tested in this study. The creep model used here is the power law proposed by Findley (Findley et al., 1976; Findley, 1960). This model is reasonably simple and has been proven to apply to a variety of viscoelastic materials loaded at moderate levels, including fiber reinforced plastics. In addition, this model has been validated by creep tests with a total duration of up to 26 years (Findley, 1987). A

full description of the stress dependent and stress independent power law proposed by Findley can be found in Kobbe (2005).

### **C.3 Materials and Methods**

The material investigated was a polypropylene wood-plastic composite. Solid deck board specimens (1-in. (2.54-cm) by 5.5-in. (13.97-cm)) were produced using a conical counter-rotating twin-screw extruder. All specimens were composed of a polypropylene (PP) based formulation consisting of 58.8-percent pine (*Pinus* spp.) flour (60-mesh, Amercian Wood Fibers 6020), 33.8-percent polypropylene (PP) matrix resin (Solvay HB9200), 4-percent talc (Luzenac Nicron 403), 2.3-percent maleic anhydride polypropylene (MAPP) coupling agent (Honeywell 950P), and 1.0-percent lubricant (Honeywell OP100) by weight. From previous static bending tests (Slaughter, 2004) the mean flexural mechanical properties were found to be: ultimate strain ( $\epsilon_{\text{failure}}$ ) = 0.012-in/in (mm/mm); modulus of elasticity (MOE) = 794,081-psi (5475.0-MPa), and modulus of rupture (MOR) = 6,494-psi (44.8-MPa).

Twenty-four test frames, operated within a controlled environment, were used for flexure creep tests. The frames were designed to conduct weak-axis flexural creep. Each frame has a support span of 24 inches (0.61-m), and two equal point loads were applied at the third points (8-in. (20.3-cm) from the support). Weights, used to supply the specified constant stress, were hung from a pulley providing an approximate 8:1 mechanical advantage. Each specimen was subjected to a constant load for 26 days. Center span displacement was measured with a linear position transducer. Data acquisition software recorded displacement and time values throughout the test.

Loads were determined from static bending test data. The focus was to determine if the material is linearly viscoelastic at stresses near design levels. Thus, stress levels were targeted to be near 10, 15, 25, 35, and 45-percent of the mean ultimate bending stress. Loads resulting in extreme fiber stresses of 649, 974, 1624, 2273, and 2922-psi (4.5, 6.7, 11.2, 15.7, and 20.1-Mpa) were applied to eight specimens each in five groups. These values correspond to approximately 30, 40, 70, 100, and 130-percent of the design bending stress.

Deflection data was obtained for eight specimens at each load level and an average value was calculated for each reading. The average deflection value,  $\delta$ , was then used in Equation (C1):

$$\varepsilon_{\max} = \frac{108\delta h}{23L^2} \quad (C1)$$

where:  $\delta$  = maximum mid-span deflection;  $h$  = thickness of the specimen; and  $L$  = span length, to calculate the maximum strain,  $\varepsilon_{\max}$ , in the outer fiber at the mid-span. The corresponding maximum fiber stress,  $\sigma_{\max}$ , was calculated using the relation:

$$\sigma_{\max} = \frac{PLh}{12I} \quad (C2)$$

where  $P$  = applied load and  $I$  = moment of inertia about the weak axis. Equation (C2) is a special form of the flexural formula:

$$\sigma = \frac{My}{I} \quad (C3)$$

where  $M$  = bending moment ( $PL/6$  for third point bending) and  $y$  = distance to the neutral axis (assumed to be  $h/2$ ). Equation (C1) is obtained by substituting Equation (C2) and the constitutive equation:



$$\sigma = E\varepsilon \quad (C4)$$

into the deflection equation:

$$\delta = \frac{23L^3P}{1296EI} \quad (C5)$$

#### C.4 Results and Discussion

Experimental and theoretical creep-strain curves are shown in Figure C.1. Consistent with short-term pure mode creep testing (Kobbe, 2005), predictions are formulated using both the general form of the power law as well as the stress independent model developed by Findley. The general model fit the creep parameters  $m$  and  $n$  to experimental data at each specific stress level. The initial elastic strain,  $\varepsilon_0$ , was taken as the strain recorded immediately following load application.

Table C.1 depicts values for the general power law model as well as predictions at 1, 12,000, 24,000, and 36,000-minutes. It can be seen that the results are in general agreement. The power law model deviated by no more than 1.12-percent from values obtained experimentally. Creep curves from the initial round of testing (25, 35, and 45-percent of ultimate) indicate a conditional change most likely occurred at approximately 11,000-minutes having the most noticeable effects on the heavily loaded specimens. Although testing was conducted in an environmentally controlled room (temperature = 68° F and relative humidity = 52-percent), occasional spikes in temperature and humidity were noticed in early testing. This problem was rectified for subsequent tests. The creep parameter,  $n$ , was reasonably constant at each stress level, averaging 0.246±8-percent. Defined as a material constant, it was expected that  $n$  would be comparable to compression and tension creep test parameters (Kobbe, 2005). The  $n$  value of 0.246

observed in flexure testing was 12 and 18-percent lower than the average for compression and tension testing. This variation is most likely due to the fact that this material was produced in an earlier extrusion run and tested under different environmental conditions. Values for the creep parameter,  $m$ , varied considerably depending on the applied stress level.

The stress dependent model parameters  $\varepsilon_0$  and  $m$  were replaced by the hyperbolic sine function. The constants  $\varepsilon_0'$ ,  $\sigma_\varepsilon$ ,  $m'$ , and  $\sigma_m$  were empirically determined from data collected at different stress levels. Values for  $\sigma_\varepsilon$  and  $\sigma_m$  were determined by linearizing the curves for  $\varepsilon_0$  and  $m$  obtained in tests over a range of stresses. Values for  $\varepsilon_0'$  and  $m'$  were taken as the slope of a straight-line fit through the respective data. Figures C.2 and C.3 show the parameters used to describe creep in flexure in relation to those obtained for compression and tension (Kobbe, 2005). Values for the stress independent Findley power law model as well as predictions at selected times are reported in Table C.2. The time dependent strain,  $\varepsilon_t$ , can now be represented as:

$$\text{Flexure: } \varepsilon_t = 4.40e^{-3} \sinh\left(\frac{\sigma}{3807}\right) + 1.22 \sinh\left(\frac{\sigma}{1552}\right) \left(\frac{t}{t_0}\right)^{0.246} \quad (\text{C6})$$

where:  $\sigma$  = the applied stress;  $t$  = time after loading; and  $t_0$  = unit time. Equation (C6) can now be used to estimate creep strains at various loading levels within the bounds experimental data (45-percent of the ultimate bending strength). The difference between the experimental and estimated values was typically less than 7-percent. These results indicate that Findley's power law model can be used to evaluate the time-dependent creep deformation of this material with acceptable accuracy.

Figure C.4 compares creep compliance values for stresses ranging from 649-2,922-psi (4.5-20.1 MPa). Evaluation of the compliance data indicates that this material

behaves non-linearly even at low stress levels. Figure C.5 illustrates values for creep compliance evaluated at intervals between 1 and 36,000-minutes following load application. Evaluating the compliance and stress data as a function of time shows that compliance is stress dependent at all stress levels. This figure also illustrates how compliance increases rapidly early in the test but begins to stabilize as the test progresses. This is an expected response for a material entering the secondary stage of creep.

Serviceability is a frequent concern for the wood-plastic composite industry. These tests indicate similar issues. Immediately after load application, deflections were  $L/268$ ,  $L/172$ ,  $L/100$ ,  $L/69$ , and  $L/53$ . After 26 days, the deflections had increased to  $L/142$ ,  $L/90$ ,  $L/46$ ,  $L/29$ , and  $L/19$ . These deflections correspond to stress levels of 10, 15, 25, 35, and 45-percent of MOR, respectively. Where  $L$  is the clear span of the specimen and is equal to 24 inches.

## **C.5 Conclusions**

Findley's power law has proven to be a successful model for creep behavior of this material. Using Findley's stress-independent model, time-dependent strain was predicted with accuracies that are generally acceptable in civil engineering. An important restriction to this model is that it cannot describe non-linear tertiary creep; therefore stress levels must be kept sufficiently low to avoid this stage of creep. Test results indicate that this material will behave in a non-linear viscoelastic nature for all practical load levels. Further testing will be needed to ensure that the secondary creep phase can be maintained at these stress levels. Serviceability may prove to be the limiting factor in

some structural applications; therefore, designers must allow appropriate consideration of this material's inherent strengths and weaknesses.

## C.6 References

- Findley, W.N., "Mechanisms and Mechanics of Creep of Plastics." SPEJ, Vol. 16, pp. 57-65, January 1960.
- Findley, W.N., Lai, J.S., and Onaran, K., "Creep and Relaxation of Nonlinear Viscoelastic Materials." North-Holland Publishing Company, New York, NY, 1976.
- Findley, W.N., "26-year Creep and Recovery of Polyvinylchloride and Polyethylene." Polymer Engineering and Science, Vol. 27, No. 8, pp. 582-585, 1987.
- Flugge, W., "Viscoelasticity." Blaisdell, Waltham, MA, 1967.
- Fung, Y.C., "Foundations of Solid Mechanics." Prentice Hall, Englewood Cliffs, NJ, 1965.
- Jazouli, S., Luo, W., Bremand, F., and Vu-Khanh, T., "Application of Time-stress Equivalence to Nonlinear Creep of Polycarbonate." Polymer Testing, Vol. 24, pp. 463-467, 2005.
- Kobbe, R.G., "Creep Behavior of Wood-Polypropylene Composites." Chapter 3, Master Thesis, Washington State University, June 2005.
- Lou, Y.C. and Schapery, R.A., "Viscoelastic Characterization of a Nonlinear Fiber-Reinforced Plastic," Journal of Composite Materials, Vol. 5, pp. 208-234, 1971.
- Rand, J.L., "A Nonlinear Viscoelastic Creep Model." Tappi Journal. Pp. 178-182, July 1995.
- Schapery, R.A., "On the Characterization of Nonlinear Viscoelastic Materials." Polymer Engineering and Science, Vol. 9, No. 4, pp. 295-310, 1969.
- Slaughter, A.E., "Design and Fatigue of a Structural Wood-Plastic Composite." Master Thesis, Washington State University, August 2004.

## C.7 Tables

**Table C.1.** Measured strain compared to predictions derived with the general power law.

	Creep Parameters <sup>a</sup>					Average Creep Strain (%) at Time t (min)				
Loading Mode	Stress (psi)	$\epsilon_0$ (%)	m ( $\epsilon$ )	n	$r^2$	t=1	t=12,000	t=24,000	t=36,000	Ave. Error
Flexure	Predictions using Findley's General Model									
	2922	0.370	0.039	0.263	0.985	0.410	0.835	0.928	0.991	-1.12%
	2273	0.281	0.025	0.259	0.984	0.306	0.566	0.622	0.659	-0.83%
	1624	0.194	0.014	0.260	0.985	0.208	0.358	0.390	0.412	-0.84%
	974	0.113	0.009	0.229	0.990	0.122	0.192	0.206	0.215	-0.82%
	649	0.072	0.006	0.222	0.985	0.078	0.119	0.127	0.132	-0.20%
	Experimental Measurements									
	2922					0.396	0.876	0.961	0.991	
	2273					0.297	0.588	0.641	0.657	
	1624					0.202	0.370	0.402	0.412	
	974					0.119	0.200	0.209	0.215	
	649					0.076	0.118	0.128	0.136	

<sup>a</sup> Average of 8 results.

**Table C.2.** Measured strain compared to predictions derived with Findley's power law.

	Creep Parameters <sup>a</sup>					Average Creep Strain (%) at Time t (min)				
Loading Mode	Stress (psi)	$\epsilon_0$ (%)	$\epsilon_0'$	$m'$ ( $\epsilon$ )	n	t=1	t=12,000	t=24,000	t=36,000	Ave. Error
Flexure	Predictions using Findley's Model									
	2922	0.370	0.332	0.012	0.246	0.417	0.777	0.852	0.902	-6.60%
	2273	0.281	0.332	0.012	0.246	0.301	0.529	0.576	0.607	-6.61%
	1624	0.194	0.332	0.012	0.246	0.204	0.341	0.369	0.388	-5.23%
	974	0.113	0.332	0.012	0.246	0.118	0.191	0.206	0.216	-1.85%
	649	0.072	0.332	0.012	0.246	0.078	0.124	0.134	0.141	3.67%
	Experimental Measurements									
	2922					0.396	0.876	0.961	0.991	
	2273					0.297	0.588	0.641	0.657	
	1624					0.202	0.370	0.402	0.412	
	974					0.119	0.200	0.209	0.215	
	649					0.076	0.118	0.128	0.136	

<sup>a</sup> Average of 8 results.

## C.8 Figures

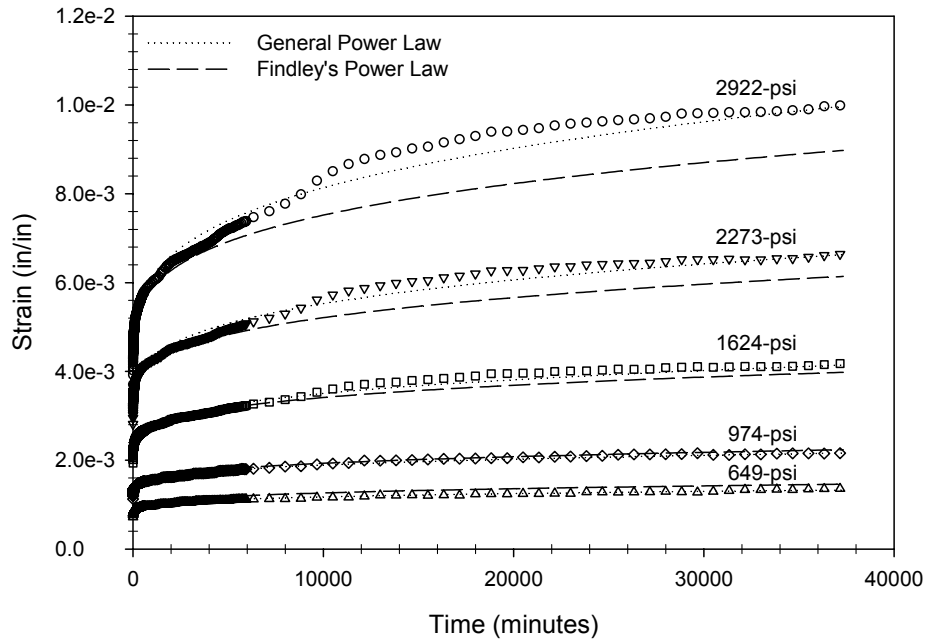


**Fig. C.1.** Measurements and predictions for creep strain in flexure.



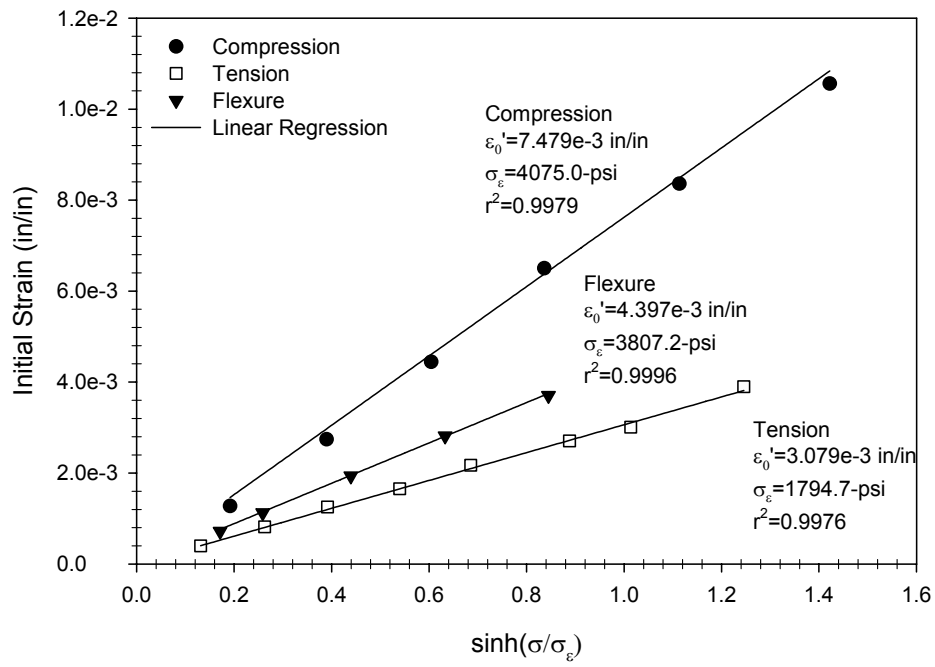


**Fig. C.2.** Evaluation of creep parameters  $\epsilon_0'$  and  $\sigma_\epsilon$ .

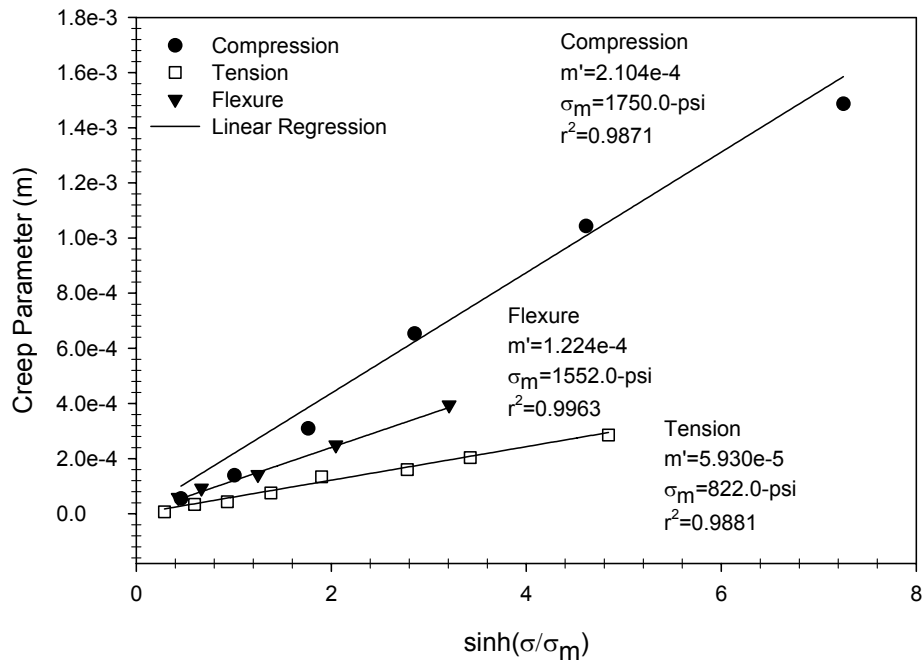


**Fig. C.3.** Evaluation of creep parameters  $m'$  and  $\sigma_m$ .

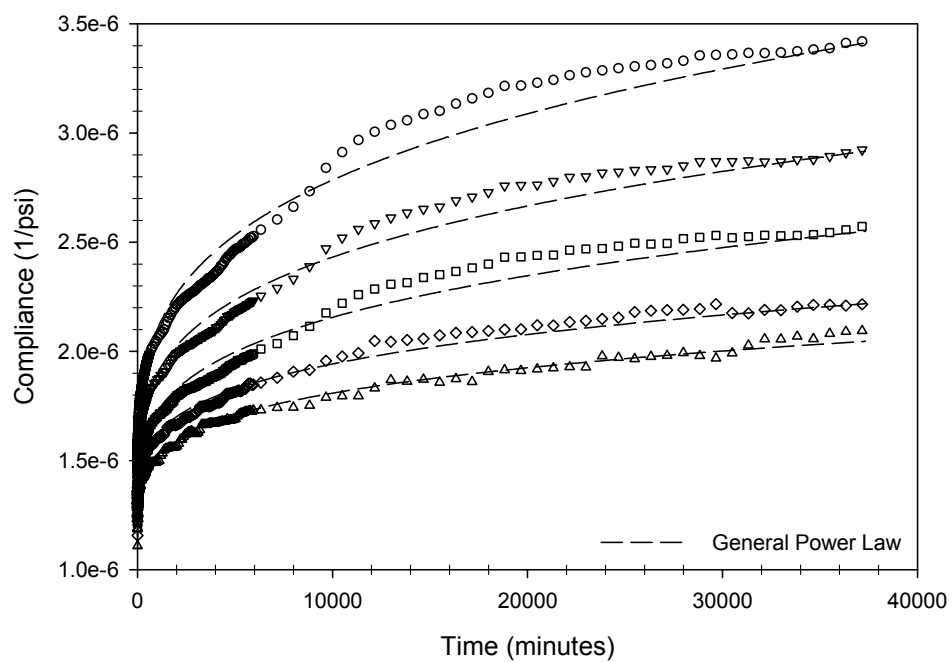


**Fig. C.4.** Creep compliance measurements for flexure.

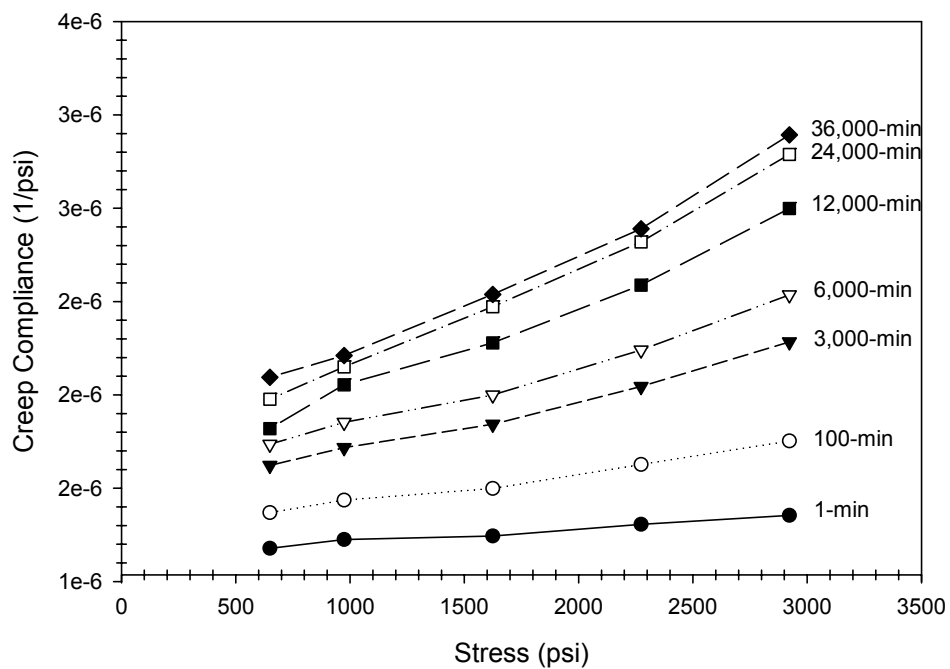


**Fig. C.5.** Creep compliance measurements at various times throughout the test.